

Polarizability of ultracold Rb₂ molecules in the rovibrational ground state of a³Σ_u⁺

Markus Deiß, Björn Drews, and Johannes Hecker Denschlag

*Institut für Quantenmaterie and Center for Integrated Quantum Science and Technology IQST,
Universität Ulm, 89069 Ulm, Germany*

Nadia Bouloufa-Maafa, Romain Vexiau, and Olivier Dulieu

*Laboratoire Aimé Cotton, CNRS, Université Paris-Sud, ENS Cachan,
Bât. 505, Campus d'Orsay, 91405 Orsay Cedex, France*

(Dated: December 7, 2024)

Abstract

We study, both theoretically and experimentally, the dynamical polarizability $\alpha(\omega)$ of Rb₂ molecules in the rovibrational ground state of a³Σ_u⁺. Taking all relevant excited molecular bound states into account, we compute the complex-valued polarizability $\alpha(\omega)$ for wave numbers up to 20000 cm⁻¹. Our calculations are compared to experimental results at 1064.5 nm ($\sim 9400 \text{ cm}^{-1}$) as well as at 830.4 nm ($\sim 12000 \text{ cm}^{-1}$). Here, we discuss the measurements at 1064.5 nm. The ultracold Rb₂ molecules are trapped in the lowest Bloch band of a 3D optical lattice. Their polarizability is determined by lattice modulation spectroscopy which measures the potential depth for a given light intensity. Moreover, we investigate the decay of molecules in the optical lattice, where lifetimes of more than 2 s are observed. In addition, the dynamical polarizability for the X¹Σ_g⁺ state is calculated. We provide simple analytical expressions that reproduce the numerical results for $\alpha(\omega)$ for all vibrational levels of a³Σ_u⁺ as well as X¹Σ_g⁺. Precise knowledge of the molecular polarizability is essential for designing experiments with ultracold molecules as lifetimes and lattice depths are key parameters. Specifically the wavelength at $\sim 1064 \text{ nm}$ is of interest, since here, ultrastable high power lasers are available.

I. INTRODUCTION

Owing to the extraordinary control over the internal and external degrees of freedom, ultracold molecules trapped in an optical lattice represent a system with many prospects for studies in ultracold physics and chemistry [1, 2], the realization of molecular condensates [3], precision measurements of fundamental constants [4–7] and quantum computation [8, 9] and simulation [10]. In the recent years, several groups have realized the preparation of optically trapped vibrational ground state ($v = 0$) molecules in either the lowest lying singlet or triplet potential [11–15]. Experiments with these molecules, e.g. ultracold collisions, are typically carried out in optical lattices or optical dipole traps [16–18]. In these environments, precise knowledge of the dynamical polarizability of molecules is a prerequisite for well controlled experiments.

The Rb₂ molecule is one of the few ultracold molecular species currently available, with which benchmark experiments for nonpolar molecules can be carried out. Here we investigate the dynamical polarizability $\alpha(\omega)$ of a Rb₂ triplet molecule in the lowest rovibrational level of a $^3\Sigma_u^+$. A similar analysis for Cs₂ regarding the electronic ground state $X^1\Sigma_g^+$ was previously carried out by Vexiau *et al.* [19]. In addition to calculations of the frequency dependent dynamical polarizability $\alpha(\omega)$, we present measurements of the real part $\text{Re}\{\alpha(\omega)\}$ at a wavelength of $\lambda = 1064.5\text{ nm}$. The experiments are performed with molecules trapped in the lowest Bloch band of a cubic 3D optical lattice which consists of three standing light waves with polarizations orthogonal to each other. By carrying out modulation spectroscopy on one of the standing light waves, we map out the energy band-structure for various light intensities. From these measurements $\text{Re}\{\alpha(\omega)\}$ is determined. Our experimental findings at $\lambda = 1064.5\text{ nm}$ and also those at 830.4 nm [12] agree well with the calculations. In addition, we experimentally investigate the decay time of the deeply bound molecules in a 3D optical lattice at 1064.5 nm for various lattice depths. Here, lifetimes of more than 2 s are observed. Furthermore, we present numerical results for the dynamical polarizabilities of the rovibronic ground state, i.e., the lowest rovibrational level of the $X^1\Sigma_g^+$ potential. For convenient application of our results, we provide a simple analytical expression and the corresponding effective parameters which can be used to reproduce the dynamical polarizabilities for all vibrational levels of both, the lowest singlet as well as triplet state outside the resonant wavelength regions.

This article is organized as follows. In section II, we give a brief, general introduction to the dynamical polarizability $\alpha(\omega)$ of a homonuclear diatomic molecule. Sections III to VI describe the

calculations and measurements related to the polarizability of $^{87}\text{Rb}_2$ in the rovibrational ground state of $a^3\Sigma_u^+$, along with a comparison of our results to reference values from literature. In section VII we present calculations of the polarizability for the rovibrational ground state of $X^1\Sigma_g^+$. Afterwards, section VIII provides a simple expression which parametrizes the polarizability for all vibrational levels of the lowest singlet as well as triplet state. A table with the corresponding parameters can be found in the Supplemental Material [20].

II. INTERACTION OF A DIATOMIC MOLECULE WITH LIGHT

When a nonpolar molecule is subject to a linearly polarized electric field $\vec{E} = \hat{\epsilon}E_0\cos(\omega t)$ with amplitude E_0 and unit polarization vector $\hat{\epsilon}$, a dipole moment $\vec{p} = \overleftrightarrow{\alpha}(\omega)\vec{E}$ is induced. In general, $\overleftrightarrow{\alpha}(\omega)$ is a tensor (see, e.g., [21]). For the sake of simplicity, we restrict ourselves to molecules in a given vibrational level v of a molecular state and in the lowest rotational level $N = 0$ of the nuclei, for which only the scalar isotropic polarizability $\alpha(\omega)$ is relevant. Here, $\vec{N} = \vec{L} + \vec{R}$, where \vec{L} denotes the total electronic angular momentum and \vec{R} is the mechanical rotation of the atomic pair. The complex dynamical polarizability characterizes the response of a molecule to the electric field expressed by photon scattering and the ac Stark shift of molecular levels. This shift is directly linked to the dipole interaction potential

$$U = -\langle \vec{p} \cdot \vec{E} \rangle / 2 = -\frac{1}{4} \text{Re}\{\alpha(\omega)\} E_0^2 \quad (1)$$

and therefore to the real part of the polarizability $\text{Re}\{\alpha(\omega)\}$ (see, e.g., [22]). In Eq. (1), the angled brackets $\langle \dots \rangle$ indicate time averaging. We note, that the dipole potential is attractive, when the sign of $\text{Re}\{\alpha(\omega)\}$ is positive and repulsive otherwise. The imaginary part of the polarizability $\text{Im}\{\alpha(\omega)\}$ is related to the power P_{abs} absorbed by the oscillator from the driving field, since

$$P_{\text{abs}} = \langle \dot{\vec{p}} \cdot \vec{E} \rangle = \frac{1}{2} \omega \text{Im}\{\alpha(\omega)\} E_0^2. \quad (2)$$

We calculate the dynamical polarizability $\alpha(\omega)$ following the method described in Ref. [19]. The generic expression of the polarizability for a diatomic molecule in a state $|i\rangle$ is

$$\alpha(\omega) = \frac{2}{\hbar} \sum_f \frac{\omega_{if} - i\frac{\gamma_f}{2}}{\left(\omega_{if} - i\frac{\gamma_f}{2}\right)^2 - \omega^2} \left| \langle f | \vec{d} \cdot \hat{\epsilon} | i \rangle \right|^2. \quad (3)$$

Here, the angled brackets refer to the spatial integration over all internal coordinates of the system. The summation covers all the accessible dipole transitions with frequency ω_{if} and transition

electric dipole moment \vec{d} from the initial state $|i\rangle$ to final states $|f\rangle$ with line width γ_f .

III. CALCULATION OF $\alpha(\omega)$ FOR $a^3\Sigma_u^+$ MOLECULES

A. Relevant transitions

If the molecule is initially in a vibrational level v_a of the $a^3\Sigma_u^+$ state, all rovibrational levels (including the continuum) of the electronic potentials with ${}^3\Sigma_g^+$ and ${}^3\Pi_g$ symmetry need to be accounted for in Eq. (3). As $N = 0$ in the initial $a^3\Sigma_u^+$ state, only transitions towards final levels with total angular momentum $J = 0, 1, 2$ must be considered. Here, $\vec{J} = \vec{S} + \vec{N}$, where \vec{S} is the total electronic spin. Therefore, when considering a diatomic molecule it is usual to define two contributions to the isotropic polarizability α : the parallel polarizability α_{\parallel} along the molecular axis \hat{Z} , which is related to d_Z , and the perpendicular polarizability α_{\perp} , which is related to $d_X = d_Y$. In general, α_{\parallel} involves ${}^3\Sigma^+ \rightarrow {}^3\Sigma^+$ transitions and α_{\perp} is related to ${}^3\Sigma^+ \rightarrow {}^3\Pi$ transitions. One can show that $\alpha = (\alpha_{\parallel} + 2\alpha_{\perp})/3$ (see, e.g., Refs. [19, 21]).

The expression given by Eq. (3) deals only with the transitions involving the two valence electrons of Rb_2 . Following Ref. [23], the contribution to the polarizability of the two Rb^+ cores, hereafter referred to as α_c , must be taken into account, and is added to the results of Eq. (3). More details about this quantity are discussed in Appendix A.

The first step of the calculations is to collect a set of accurate molecular potential energy curves (PECs) and transition electric dipole moments (TEDMs). The $a^3\Sigma_u^+$ PEC is taken from the spectroscopic study of Ref. [24]. For the excited molecular states and the related TEDMs from the $a^3\Sigma_u^+$ state, we use the same data as Refs. [25, 26], which we report in the Supplemental Material [20] attached to the present paper, for convenience. The PECs are displayed in Fig. 1, while the TEDMs are drawn in Appendix B. These data are obtained by the quantum chemistry approach described in details in Ref. [27]. Briefly the Rb_2 molecule is considered as two valence electrons moving in the field of the two ionic Rb^+ cores, which are represented by a large effective core potential (ECP) including a core polarization potential (CPP) [28, 29]. A full configuration interaction (FCI) is then performed on the two valence electrons, using a large gaussian basis set [30], with the CIPSI quantum chemistry code developed at Université Paul Sabatier in Toulouse. It is worth mentioning that partial spectroscopic information is available on the ${}^1\Sigma_g^+$ [31] and the ${}^1\Pi_g$ [32] state, but no complete PEC has been extracted in these studies. As discussed for instance in

Refs. [26, 32], the computed PECs are suitable to reproduce the observed data provided that they are slightly shifted in frequency (in terms of $\omega/2\pi c$, by at most 100 cm^{-1}). However, as it will be discussed later on, such shifts only have negligible consequences on the results reported in the present paper. Finally, the vibrational wave functions of levels $|i\rangle$ and $|f\rangle$ for the summation are obtained using the Mapped Fourier Grid Hamiltonian representation [33, 34].

B. Results

The real and imaginary parts of the dynamical polarizability $\alpha_{v_a=0}(\omega)$ of a molecule in the vibrational ground state of the $a^3\Sigma_u^+$ potential are displayed in Fig. 1(b) and (c) as functions of the trapping laser frequency. The polarizabilities are expressed in atomic units (a.u.), which can be converted into SI units according to $1\text{ a.u.} = 4\pi\varepsilon_0 a_0^3 = 1.649 \times 10^{-41}\text{ J m}^2\text{ V}^{-2}$, where a_0 denotes the Bohr radius and ε_0 is the vacuum permittivity. Note, for some applications, e.g., considerations related to the ac Stark shift, units of $\text{Hz W}^{-1}\text{ cm}^2$ (1 a.u. corresponds to $4.6883572 \times 10^2 \text{ Hz W}^{-1}\text{ cm}^2$) are advantageous. The sum in Eq. (3) has been truncated to include only the vibrational levels of the four lowest ${}^3\Sigma_g^+$ states and the three lowest ${}^3\Pi_g$ states. While it is difficult to provide a strict error bar, we checked that adding a couple of upper electronic states in the sum of Eq. (3) contributes to the polarizability for less than 1%. The associated molecular data are collected in the Supplemental Material [20]. For simplicity, the natural lifetime $\tau_f = (\gamma_f)^{-1}$ has been fixed to 10 ns ($\gamma_f \approx 2\pi \times 15\text{ MHz}$) for all the excited molecular levels. As discussed below (see experimental section), this is a reasonable approximation. Strongly oscillating patterns in both $\text{Re}\{\alpha_{v_a=0}(\omega)\}$ and $\text{Im}\{\alpha_{v_a=0}(\omega)\}$ [see Figs. 1(b) and (c), respectively] correspond to frequency ranges of strong absorption which should be disregarded for trapping purpose. The real part smoothly increases from the static polarizability $\alpha_{v_a=0}(\omega = 0) = 698.5\text{ a.u.}$ up to the bottom of the ${}^1\Sigma_g^+$ potential well, reaching 3147 a.u. at the wavelength of the trapping laser used in the present experiment (1064.5 nm). In the same region the imaginary part increases from about 10^{-5} a.u. at $\omega = 0$ to 10^{-3} a.u. at the trapping laser frequency which leads to a correspondingly larger photon scattering rate.

IV. MEASUREMENT OF $\text{Re}\{\alpha(\omega)\}$ FOR $a^3\Sigma_u^+$

A. Experimental setup and measurement scheme

The experiments presented in this work are carried out with a pure sample of about 1.5×10^4 ${}^{87}\text{Rb}_2$ molecules prepared in the rovibrational ground state of the $a^3\Sigma_u^+$ potential and trapped in a

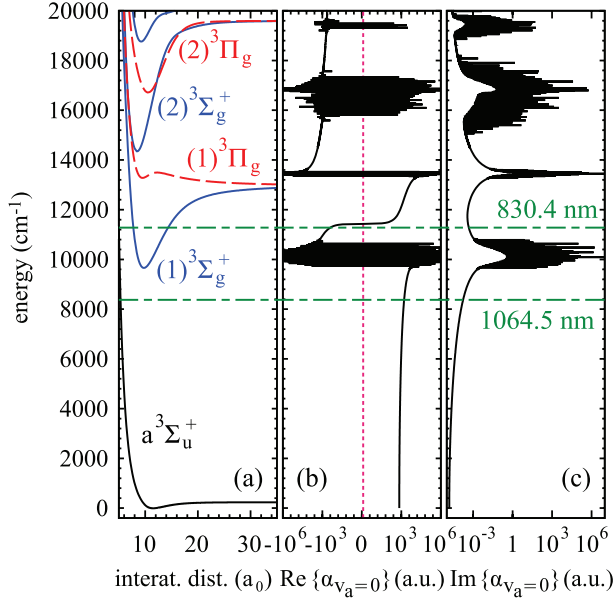


FIG. 1. (Color online) (a) $^3\Sigma_g^+$ (solid blue lines) and $^3\Pi_g$ (dashed red lines) potential curves of Rb_2 [25, 26]. The $a^3\Sigma_u^+$ potential is drawn in black. In (b) and (c) the real and imaginary parts of the dynamical polarizability $\alpha_{v_a=0}$ of Rb_2 molecules in the rovibrational ground level ($v_a = 0, R = 0$) of the $a^3\Sigma_u^+$ molecular state are shown as a function of $\omega/(2\pi c)$. The two wavelengths used in the experiments are indicated by dashed horizontal lines. Furthermore, the red dashed vertical line in (b) represents zero polarizability.

3D optical lattice. There is no more than a single molecule per lattice site and the temperature of the sample is about $1 \mu\text{K}$. As described in detail in Refs. [12, 21, 35], the molecules are prepared as follows. An ultracold thermal cloud of spin-polarized ^{87}Rb atoms ($f_{\text{Rb}} = 1, m_{f,\text{Rb}} = 1$) is adiabatically loaded into the lowest Bloch band of a 3D optical lattice at a wavelength of $\lambda = 1064.5 \text{ nm}$. The lattice is formed by a superposition of three linearly polarized standing light waves with polarizations orthogonal to each other, see Fig. 2(a). The three lattice beams are derived from the same laser source with a linewidth of a few kHz and have relative intensity fluctuations of less than 10^{-3} . In order to avoid interference effects, the frequencies of the standing waves are offset by about 100 MHz relative to each other. At the location of the atomic sample the beam waists ($1/e^2$ radii) are about $130 \mu\text{m}$ and the maximum available power per beam is about 3.5 W. By slowly crossing the magnetic Feshbach resonance at 1007.4 G we produce weakly bound diatomic molecules. After a purification step which removes remaining atoms, a STIRAP (stimulated Raman adiabatic passage) is performed at 1000 G, transferring the dimers into the rovibrational ground state ($v_a = 0, N = 0, m_N = 0$) of the $a^3\Sigma_u^+$ potential. Here, m_N is the projection

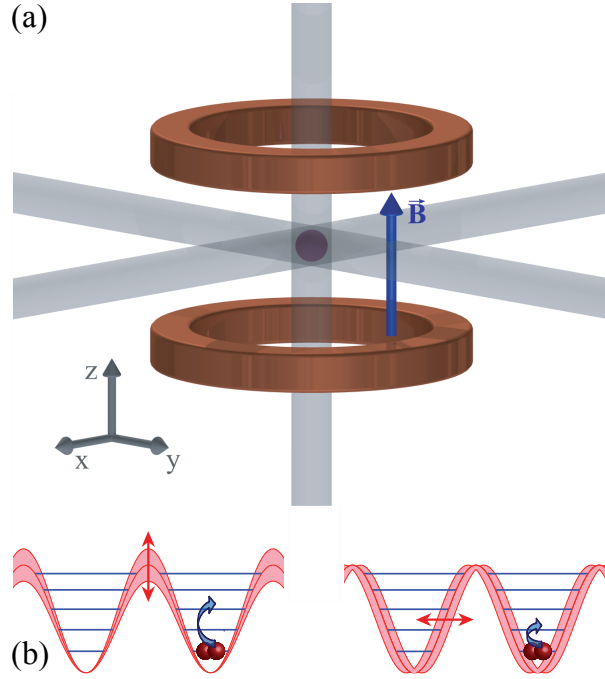


FIG. 2. (Color online) (a) Experimental scheme. Three retroreflected laser beams with polarizations orthogonal to each other form a 3D optical lattice. A trapped cloud of Rb_2 molecules is sketched in the intersection of the laser beams. The optical lattice is located between two Helmholtz coils which create a magnetic field \vec{B} . In our setup, the direction of \vec{B} represents the quantization axis. (b) Illustration of amplitude (left) and phase (right) modulation spectroscopy.

on the quantization axis defined by the direction of the magnetic field \vec{B} [cf. Fig. 2(a)]. The molecule has positive total parity, total electronic spin $S = 1$, total nuclear spin $I = 3$ and is further characterized by the quantum number $f = 2$ ($\vec{f} = \vec{S} + \vec{I}$). Moreover, the total angular momentum is given by $F = 2$ ($\vec{F} = \vec{f} + \vec{J}$) and its projection is $m_F = 2$. Henceforth, we simply refer to these molecules as "v_a = 0 molecules".

According to Eq. (1), $\text{Re}\{\alpha(\omega)\} = 4|U|/E_0^2$, i.e., the real part of the dynamical polarizability can be determined by measurements of the potential depth $|U|$ and the electric field amplitude E_0 of an optical trap. For the case of a cubic 3D optical lattice with orthogonal polarizations, the trapping potential is given by $V(x, y, z) = \sum_{\beta=x,y,z} V_\beta(\beta)$ where the

$$V_\beta(\beta) = -|U|_\beta \cos^2(k\beta + \phi_\beta) \quad (4)$$

represent the contributions of the standing waves of directions $\beta = x, y, z$ with $k = 2\pi/\lambda$ being the wave number of the lattice beams. We now only consider the part of the lattice in the vertical z

direction since this axis is the only one relevant for the measurements of the potential depth in the present work. Therefore, we define $V_z(z) \equiv V(z)$, $|U|_z \equiv |U|$ and $\phi_z \equiv \phi$. The phase ϕ is a function of the laser wavelength λ because the standing light wave is created by retroreflecting the laser beam from a fixed mirror at position z_m . It is given by $\phi = 4\pi z_m / \lambda$ at $z = 0$.

B. Lattice modulation spectroscopy

In order to obtain $|U|$, we carry out lattice modulation spectroscopy (see, e.g. [13, 36–38]). For this, we either modulate $|U|$ by periodically changing the intensity of the standing light wave (amplitude modulation) or we modulate the phase ϕ by periodically changing the laser wavelength λ (phase modulation). Resonant amplitude (phase) modulation drives transitions from the lowest Bloch band ($n = 0$), in which the molecules have been initially prepared, to even (odd)-numbered excited lattice bands [see Fig. 2(b)]. This can cause either direct loss from the trap owing to heating (see, e.g., [36]) or molecules in higher lattice bands collide with each other and those of the lowest Bloch band, respectively, resulting in decay to nonobservable states. In consequence, resonant excitation leads to a decreased molecular signal in our measurements.

For amplitude modulation spectroscopy, we modulate the intensity of the lattice laser beam sinusoidally by a few percent. When performing phase modulation spectroscopy we modulate the laser frequency by a few MHz corresponding to a phase difference on the order of a few 10^{-2} rad as $z_m \sim 0.4$ m. The modulation duration is typically on the order of 1 ms. At the end of each experimental cycle (which takes about 40 s), the remaining number N of molecules is measured. We only find molecules in the lowest Bloch band, not in higher bands. In order to determine the molecule number, we reverse the STIRAP and dissociate the resulting Feshbach dimers by sweeping over the Feshbach resonance. Then, the generated atoms are detected via absorption imaging. By comparing the resonant transition frequencies observed in the modulation spectra to the energy band-structure of the sinusoidal lattice, the lattice depth $|U|$ is deduced. This will be explained in detail further below.

Figure 3 shows measured excitation spectra of Feshbach (a) and $v_a = 0$ (b,c) molecules, obtained via amplitude or phase modulation spectroscopy. A single data point typically consists of 5 to 30 repetitions of the experiment (For a given spectrum the number of repetitions is constant). Fig. 3(a) as well as (b) exhibit a prominent resonance after amplitude modulation. This resonance is related to a transition from the lowest Bloch band ($n = 0$) to the second excited lattice band ($n = 2$). Spectrum (a) for Feshbach molecules in addition shows a broad shoulder at around

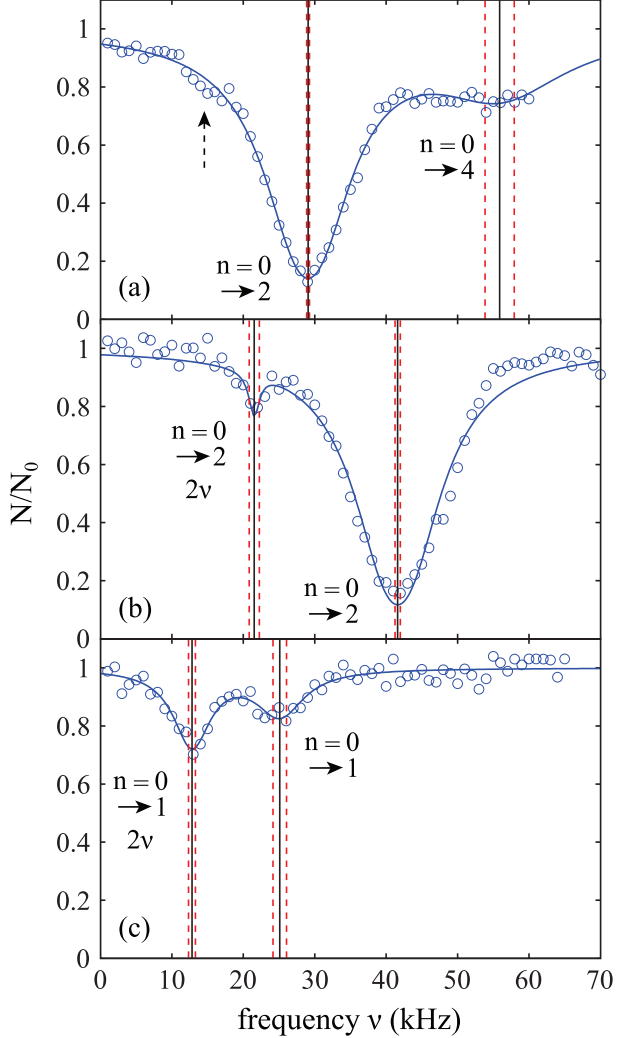


FIG. 3. (Color online) Amplitude [(a) and (b)] and phase (c) modulation spectra of weakly bound Feshbach molecules (a) and molecules in the rovibrational ground state of the $a^3\Sigma_u^+$ potential [(b) and (c)]. We measure the fraction of remaining molecules N/N_0 as a function of the modulation frequency ν . The statistical error of each data point is in the range of $\pm(0.05 - 0.15)$. Here, the numbers N_0 are given by the asymptotic limits of Lorentzian fits (solid blue lines). The resulting center frequencies of the resonances are illustrated as black vertical lines, while the red dashed lines indicate the corresponding uncertainties. We note, that the mean intensity of the lattice beam used for modulation in (b) is 30% less than in (a) and (c).

50 kHz which we attribute to a resonant transition from $n = 0$ to $n = 4$. Due to the large width of this resonance the uncertainty in the determination of its center frequency is relatively large. Spectrum (b) in Fig. 3 also features a second resonance dip, but here it is located at about half the frequency of the prominent one. This resonance dip can be assigned to a transition from the

lowest Bloch band to the second excited band, involving two identical “quanta” with frequency ν . It is known (see, e.g., [36]) that such subharmonic resonances exist. To be consistent, a similar sub-harmonic resonance dip should be present in Fig. 3(a) at about 15 kHz (as indicated by the vertical, dashed arrow). Indeed, at that position the data points seem to be systematically below the fit curve with respect to the prominent peak. However, the corresponding signal (if at all) is very weak, partially due to its position at the steep flank of the prominent resonance.

Now, we turn to Fig. 3(c), which shows an excitation spectrum after phase modulation for $v_a = 0$ molecules. We observe two resonances of similar strength, both of which we attribute to the transition from $n = 0$ to $n = 1$. The dip at lower frequency is again a subharmonic resonance. Surprisingly, it is stronger than the harmonic one at about 25 kHz. However, we have verified the assignment by comparison to the corresponding amplitude modulation spectra.

We calculate the Bloch bands by diagonalizing the Hamilton operator for the lattice in 1D (neglecting gravitation),

$$H = -\frac{\hbar^2}{2m} \frac{\partial^2}{\partial z^2} + V(z), \quad (5)$$

which is particularly simple in momentum space (see, e.g., [39]). Here, m is the mass of a molecule, i.e., twice the mass of a ^{87}Rb atom. Figure 4 shows the calculated energy eigenvalues as a function of the lattice depth. The energies are given in terms of the recoil energy $E_R = \hbar^2/(2m\lambda^2)$, with \hbar being Planck’s constant. As we do not specify the quasimomentum, the energy eigenvalues form bands which are broad for low lattice depths. However, the bands $n = 0$ to $n = 2$ are quite narrow for lattice depths above $\sim 40 E_R$. This is the regime where we take most of our measurements. Having measured the resonant excitation frequencies after modulation we could in principle use Fig. 4 to read off the corresponding lattice depth $|U|$. We refine this method and at the same time check for consistency as follows.

In the experiment we control the lattice depth $|U|$ via the laser beam power P that can be measured using photodiodes. The square to the electrical field E_0^2 is proportional to P . Consequently $|U| \propto P$, i.e., the precise value of $|U|$ is known up to a calibration factor (which depends linearly on the dynamical polarizability). Thus, given a molecular state, we should be able to adjust the calibration factor such that all data obtained for various powers P match the band structure calculation. The measured data points in Fig. 4 clearly show that this works quite well, both for deeply bound molecules (red) and Feshbach molecules (blue). In this procedure we do not account for the transitions from $n = 0$ to $n = 4$ owing to the large uncertainties of the corresponding resonances in

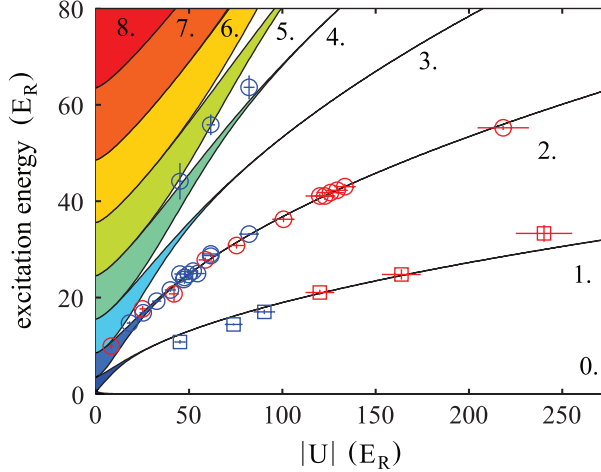


FIG. 4. (Color online) Energy band-structure with zero energy corresponding to the center of the lowest Bloch band. Solid lines are calculations for a single lattice direction, where the numbers 1. to 8. give the band index n . The data points are obtained excitation energies for $\lambda = 1064.5\text{ nm}$, stemming from amplitude (circles) or phase (squares) modulation spectroscopy. Red (blue) plot symbols indicate measurements for triplet rovibrational ground state (Feshbach) molecules. Here, the experimental results are shown after independently fitting the data for each molecular species to the band-structure calculation. By doing so, we determine the individual calibration factors and therefore the lattice depths $|U|$ (see also text). The horizontal error bars represent the resulting uncertainties of $|U|$, whereas the vertical error bars are given by the uncertainties of the Lorentzian fits in the modulation spectra.

the excitation spectra. Nevertheless, these data points are shown in the plot for comparison.

In addition to $|U|$, the electrical field amplitude E_0 of the optical lattice has to be determined in order to infer the dynamical polarizability $\alpha(\omega)$ [see Eq. (1)]. We can circumvent this by referencing the measurements on the lattice depth $|U|$ for the molecules in the rovibrational ground state of the $a^3\Sigma_u^+$ potential to similar measurements with Feshbach molecules, of which the polarizability $\alpha_{\text{Fesh}}(\omega)$ is known to be twice the one of a Rb atom $\alpha_{\text{Rb}}(\omega)$ in the electronic ground state [19]. According to Eq. (1) the lattice depths $|U_{v_a=0}|$ and $|U_{\text{Fesh}}|$ for the $v_a = 0$ and Feshbach molecules are related by

$$\frac{|U_{v_a=0}|}{|U_{\text{Fesh}}|} = \frac{\text{Re}(\alpha_{v_a=0})}{\text{Re}(\alpha_{\text{Fesh}})} \quad (6)$$

for a given lattice beam intensity, i.e., a given E_0 .

From our experiments at $\lambda = 1064.5\text{ nm}$ we obtain $\text{Re}\{\alpha_{v_a=0}\} = (2.5 \pm 0.1) \times \text{Re}\{\alpha_{\text{Fesh}}\}$, whereas $\text{Re}\{\alpha_{v_a=0}\} = (0.1 \pm 0.02) \times \text{Re}\{\alpha_{\text{Fesh}}\}$ was found at $\lambda = 830.4\text{ nm}$ [12]. Using our

calculated atomic values of 685.8 a.u (1064.5 nm) and 2995.9 a.u (830.4 nm) yields molecular polarizabilities $\text{Re}\{\alpha_{v_a=0}\}$ of 3430 ± 140 a.u (1064.5 nm) and 600 ± 120 a.u (830.4 nm), respectively.

V. COMPARISON OF RESULTS

Table I shows our measured and calculated polarizabilities along with results of other references. First, it should be noted that our theoretical atomic polarizabilities (including only the $5s - 5p$ and $5s - 6p$ transition frequencies from the NIST database [40] at 828.4 nm and at 1060.1 nm are in good agreement with the ones of Refs. [41, 42] which consider the $5s - 5p$ transition frequency from the NIST database, and *ab initio* values for the frequencies up to the $5s - 8p$ transitions.

We find good agreement between our theoretical (3147 a.u.) and experimental (3430 ± 140 a.u.) results for the molecular polarizability $\text{Re}\{\alpha_{v_a=0}\}$ at 1064.5 nm (see table I). In contrast, the agreement for the polarizability at 830.4 nm of our former measurements [12] (600 ± 120 a.u.) with the present calculations (875.8 a.u.) is somewhat poor. It is not clear how this discrepancy comes about. With respect to the static polarizability, i.e., $\omega = 0$, the calculations presented in this work give 698.5 a.u. (cf. Table I) for the $v_a = 0$ molecules. This value actually agrees well with the one previously reported in Ref. [46], 677.5 a.u., as it was not including the contribution of $\alpha_c \equiv 2 \times \alpha(\text{Rb}^+) = 18.2$ a.u. [41].

Figure 5 is a zoom into Fig. 1(b) showing the calculated real part of the dynamical polarizability of a $v_a = 0$ molecule (solid black lines). In addition, $\text{Re}\{\alpha(\omega)\}$ for a Feshbach molecule is plotted (dashed red lines), which is given by twice the atomic polarizability. The two wavelengths used in our experiments (830.4 nm and 1064.5 nm) are indicated as vertical green dashed lines. Outside the resonant and therefore lossy regions in Fig. 5 (vertical black bands) the two polarizability curves never cross. Thus, there is no so-called "magic" wavelength, where the ac Stark shift of the two molecular states caused by the trapping light is equal. Such state-insensitive trapping conditions can be beneficial, e.g., when converting Feshbach molecules to deeply bound states. Specifically, in Ref. [12], owing to the large difference of the dynamical polarizabilities at $\lambda = 830.4$ nm, the STIRAP transfer of Rb_2 from the Feshbach level to $v_a = 0$ populated several lattice bands.

We have again studied this issue in this work and find that population of higher lattice bands can be suppressed even in the absence of a magic wavelength when working with deep lattices. At $\lambda = 1064.5$ nm there is still a factor of 2.5 difference in polarizability between Feshbach and

TABLE I. Measured and calculated polarizabilities $\text{Re}\{\alpha\}$ in a.u. for ^{87}Rb atoms and $^{87}\text{Rb}_2$ molecules in the rovibrational ground state of $a^3\Sigma_u^+$. Here, the abbreviations "tw exp (theo)" mean "this work, experimental (theoretical)".

Species	λ (nm)	$\text{Re}\{\alpha\}$ (a.u.)	Ref.
^{87}Rb	828.4	3132 ± 3	[41]
^{87}Rb	828.4	3131.4	tw theo
^{87}Rb	830.4	2995.9	tw theo
$^{87}\text{Rb}_2$	830.4	875.8	tw theo
$^{87}\text{Rb}_2$	830.4	600 ± 120	[12], using $\alpha_{\text{Rb}} = 2995.9$ a.u.
^{87}Rb	1060.1	692.7	tw theo
^{87}Rb	1060.1	693.5 ± 0.9	[42]
^{87}Rb	1064.5	685.8	tw theo
$^{87}\text{Rb}_2$	1064.5	3147	tw theo
$^{87}\text{Rb}_2$	1064.5	3430 ± 140	tw exp, using $\alpha_{\text{Rb}} = 685.8$ a.u.
$^{87}\text{Rb}_2$	1064.5	3200 ± 500	[43]
^{87}Rb	∞	318.6 ± 0.6	[45]
^{87}Rb	∞	317.9	tw theo
$^{87}\text{Rb}_2$	∞	698.5	tw theo
$^{87}\text{Rb}_2$	∞	677.5	[46]

$v_a = 0$ molecules. For an initial (final) lattice depth of $50 E_R$ ($125 E_R$) at 1064.5 nm a calculation of the wavefunction overlap for the Bloch states shows that still 97% of the population stays in the lowest Bloch band after the STIRAP. In addition, we are able to energetically resolve the lattice bands during STIRAP as $n = 0$ and $n = 2$ are separated by about 40 kHz at $|U| = 125 E_R$ [cf. Fig. 4]. This strongly increases the selectivity of the transition (see, e.g., [47]). Indeed, in our experiments we do not observe any significant population of higher bands.

As can be seen in Fig. 5, the absolute dynamical polarizability of the triplet rovibrational ground state molecules at 1064.5 nm is about four times larger than at 830.4 nm. This is convenient since it results in a four times deeper interaction potential at the same laser intensity. For

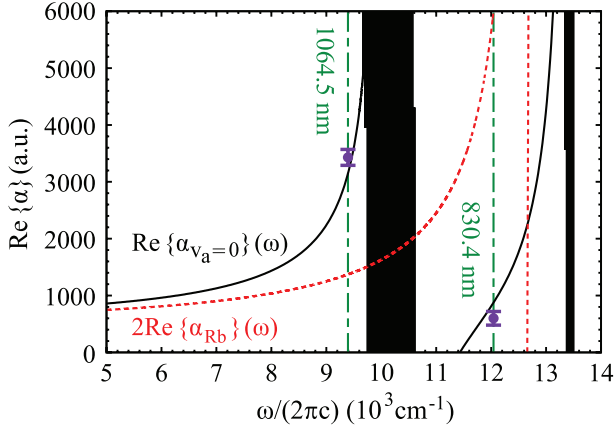


FIG. 5. (Color online) Real parts of the dynamical polarizabilities of triplet rovibrational ground state molecules (solid black lines) and Feshbach molecules (dashed red lines). The circles represent the experimental results given in Table I with the corresponding wavelengths indicated by green dashed vertical lines.

longer wavelengths than 1064.5 nm, Fig. 5 reveals, that the dynamical polarizabilities of $v_a = 0$ molecules and Feshbach molecules approach each other. Hence working at even longer wavelengths than 1064.5 nm might be advantageous for some applications.

VI. LIFETIME OF THE MOLECULES

According to Eq. (2), the imaginary part of the dynamical polarizability, $\text{Im}\{\alpha\}$, is linked to the light power absorbed by a molecule, P_{abs} , which in turn can be expressed in terms of the photon scattering rate $\Gamma_{\text{sc}} = \hbar^{-1} \omega^{-1} P_{\text{abs}}$ [22]. Using this and Eq. (1), Γ_{sc} can be written as

$$\Gamma_{\text{sc}} = -\frac{2U}{\hbar} \frac{\text{Im}\{\alpha(\omega)\}}{\text{Re}\{\alpha(\omega)\}}. \quad (7)$$

For a 3D optical lattice with equal lattice depths $|U|$ in each direction the scattering rate is given by $\Gamma_{\text{sc}}^{\text{3D}} = 3\Gamma_{\text{sc}}$. As an example, we consider the case of $|U| = 50 E_R$ at $\lambda = 1064.5 \text{ nm}$. Then, the corresponding values for the polarizability obtained in the present work, $\text{Im}\{\alpha\} = 0.96 \times 10^{-3} \text{ a.u.}$ and $\text{Re}\{\alpha\} = 3430 \text{ a.u.}$, yield $\Gamma_{\text{sc}} = 0.18 \text{ s}^{-1}$. Note, this calculation only accounts for an ideal optical lattice. As there is always background light that does not contribute to the lattice, the estimated value for the scattering rate represents just a lower bound. Once a photon is absorbed, the molecule is excited and typically decays to a nonobservable state. Assuming excitation to be

the only loss-mechanism a lifetime $\tau = 1.9$ s of the $v_a = 0$ molecules is expected in a $50 E_R$ deep 3D optical lattice at 1064.5 nm.

We experimentally investigate the lifetimes of the molecules in the rovibrational ground state of $a^3\Sigma_u^+$ by varying the holding time t_h in the lattice. Figure 6 shows lifetime measurements of $v_a = 0$ molecules for various potential depths $|U|$, which are adjusted to be equal in each direction. Applying an exponential fit, we obtain a $1/e$ decay time τ of more than 2 s for both our measurements at $|U| = 33 E_R$ and $|U| = 58 E_R$.

In order to estimate possible loss induced by inelastic molecular collisions, we calculate the tunneling rates Γ_{tu} between adjacent lattice sites within the lowest Bloch band ($n = 0$). When considering a lattice depth of $33 E_R$ ($58 E_R$) one obtains $\Gamma_{tu} = 2.37 \text{ s}^{-1}$ ($\Gamma_{tu} = 0.09 \text{ s}^{-1}$). In our setup at most 20% of the lattice sites are occupied in the region of highest molecule density. Thus, for $|U| = 33 E_R$ decay due to collisions cannot be neglected, whereas for $|U| = 58 E_R$ and beyond only loss owing to photon scattering is relevant. For such deep lattices, the lifetime τ scales directly inversely with the lattice depth $|U|$. We confirm this for the measurements at $|U_1| = 58 E_R$ and $|U_2| = 125 E_R$, since the ratio of the lifetimes $\tau_1/\tau_2 = 2.20$ is close to $|U_2|/|U_1| = 2.16$.

VII. POLARIZABILITY OF $X^1\Sigma_g^+$ MOLECULES

As the agreement between calculations and measurements for the triplet molecules is in general good, we also provide calculations for the singlet ground state of $^{87}\text{Rb}_2$. Using the same approach as above (see also [19]), we compute the dynamical polarizability $\alpha_{v_X=0}(\omega)$, i.e., with respect to the $v_X = 0, J = N = 0$ level. The $X^1\Sigma_g^+$ PEC has been derived from spectroscopic data of Ref. [48]. The $A^1\Sigma_u^+$ and the $b^3\Pi_u$ PECs and the related spin-orbit coupling between those two states are taken from Ref. [49]. The PECs for all the other states and for the TEDMs are taken from the computations reported in Refs. [25, 26]. Again, the sum in Eq. (3) has been truncated to include only the levels of the four lowest $^1\Sigma_u^+$ states and the three lowest $^1\Pi_u$ states. The natural lifetime of the excited levels has been fixed at 10 ns. Results are presented in Fig. 7, showing that two magic wavelengths can be identified at 990.1 nm and 1047.2 nm. The latter is located close to the region of strong absorption resonances and consequently, from the imaginary part [cf. Fig. 7(b)], the photon scattering rate at 1047.2 nm is expected to be by a factor of four larger than at 990.1 nm.

VIII. PARAMETRIZATION OF THE POLARIZABILITY

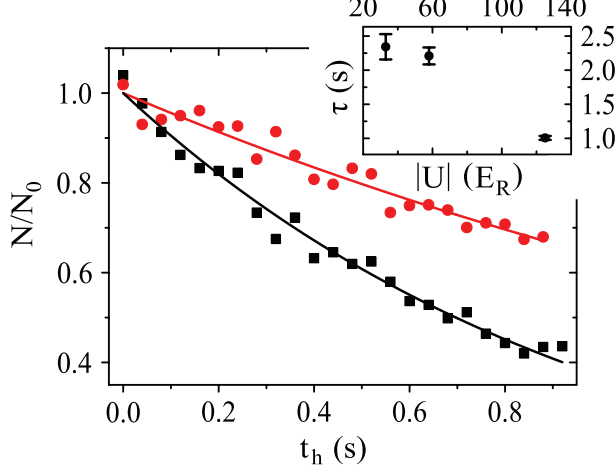


FIG. 6. (Color online) Decay of triplet rovibrational ground state molecules trapped in a 3D optical lattice at 1064.5 nm with equal potential depths of $|U|$ in each direction. Shown is the fraction of remaining molecules N/N_0 as a function of the holding time t_h in the lattice. Square plot symbols (red circles) correspond to a lattice depth of $125 E_R$ ($58 E_R$). Each data set typically consists of 10 to 15 repetitions of the experiment, where the statistical error of a data point is on the order of ± 0.1 . Solid lines are exponential fits to the data. Here, N_0 is given by the values of these fits at $t_h = 0$ s. In general, the absolute molecule numbers N_0 are about 1.5×10^4 . The inset depicts the resulting $1/e$ decay times for various lattice depths.

A. Rovibrational ground state of $a^3\Sigma_u^+$

In general, using figures (e.g., Figs. 1 and 7) to read off the dynamical polarizabilities at specific wavelengths is cumbersome. Therefore, we provide here a simple analytical fitfunction and parameters that allow for reproducing the numerical results with respect to nonresonant wavelength regimes. In the infrared and optical domain we are studying, the main contributions to the polarizability of the X (a) state outside of resonances come from the transitions towards the first excited ${}^1({}^3)\Sigma^+$ state and the first ${}^1({}^3)\Pi$ state. Thus we attempt to model the polarizability by reducing those transitions to a single effective transition towards each of the two different symmetries. The approximate real part of the polarizability is expressed as

$$\alpha_{\text{eff}}(\omega) = \frac{2\omega_\Sigma}{\hbar(\omega_\Sigma^2 - \omega^2)} d_\Sigma^2 + \frac{2\omega_\Pi}{\hbar(\omega_\Pi^2 - \omega^2)} d_\Pi^2 + \alpha_c \quad (8)$$

with ω_Σ (resp. ω_Π) the effective transition frequencies and d_Σ (resp. d_Π) the corresponding effective dipole moment. We have isolated in this expression the core polarizability α_c as its frequency dependance is much weaker than the one of the terms coming from valence electron excitation (see

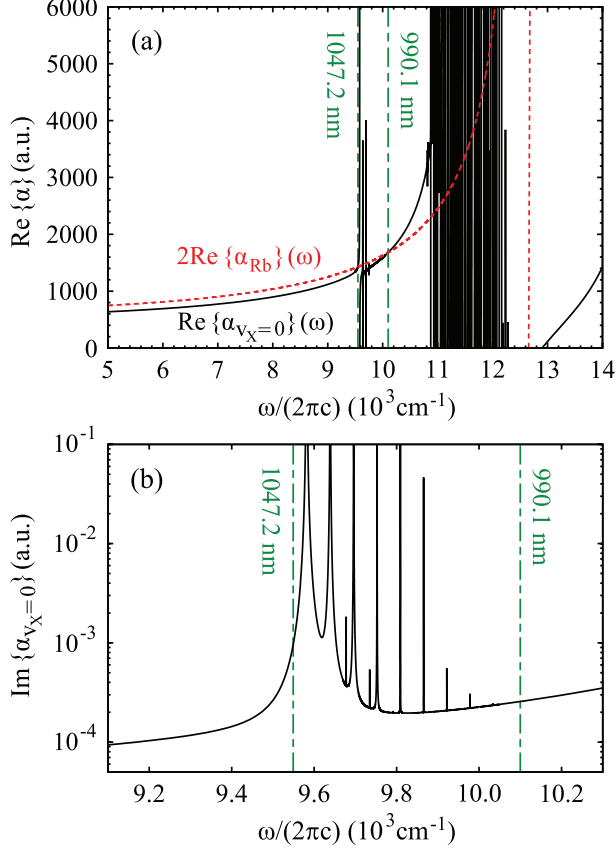


FIG. 7. (Color online) Real part (a) and imaginary part (b) of the dynamical polarizability of $^{87}\text{Rb}_2 \text{X}^1\Sigma_g^+$ molecules in their $v_X = 0, N = 0$ level. In (a), for comparison, also the numerical results corresponding to $2\text{Re}\{\alpha_{\text{Rb}}\}$ are shown (red dashed line), representing the real part of the dynamical polarizability of Feshbach molecules. Two magic wavelengths where both polarizabilities are equal are obtained and indicated by vertical dashed lines.

Appendix A). The imaginary part of the polarizability is neglected since the model is designed for the ranges outside the resonant regions.

We extract the effective parameters from a fit to the full numerical results using Eq. (8). The results with respect to the $a^3\Sigma_u^+$ and $\text{X}^1\Sigma_g^+$ rovibrational ground state are shown in Fig. 8. For the triplet case, data points with frequencies close to resonances, i.e., from $\omega/(2\pi c) = 9527 \text{ cm}^{-1}$ to 11018 cm^{-1} and above 13173 cm^{-1} , are excluded from the fit. We obtain $\omega_\Sigma/(2\pi c) = 10112.33 \text{ cm}^{-1}$, $d_\Sigma = 2.792881 \text{ a.u.}$, $\omega_\Pi/(2\pi c) = 13481.32 \text{ cm}^{-1}$ and $d_\Pi = 3.211023 \text{ a.u.}$ Note, in terms of dipole moments, atomic units can be converted into SI units according to $1 \text{ a.u.} = ea_0 = 8.478 \times 10^{-30} \text{ Ams}$. Using these parameters, the effective polarizability reproduces the numerical results in the fitted region to within a relative root mean square value (rRMS) of around 1% [see

Fig. 8(a)]. The rRMS value is defined by

$$\text{rRMS} = \sqrt{\sum_{i=1}^M \frac{1}{M} \left(\frac{\alpha_{\text{eff}}(\omega_i) - \alpha(\omega_i)}{\alpha(\omega_i)} \right)^2} \quad (9)$$

with $\alpha(\omega_i)$ being the numerical values, and $\alpha_{\text{eff}}(\omega_i)$ the fitted ones. Here, M is the number of considered values ω_i , which depends on the vibrational level as the resonant frequency regions excluded from the fit vary. We point out that if we take the transition dipole moment d_Z (resp. $d_X = d_Y$) at the equilibrium distance of the $a^3\Sigma_u^+$ state and multiply it by the appropriate Hönl-London factor ($1/\sqrt{3}$ for $\Sigma^+ - \Sigma^+$ transition and $\sqrt{2/3}$ for $\Sigma^+ - \Pi$ transition), we get the value 2.767 a.u. (resp. 3.142 a.u.), very close to the effective dipole moment found above. Moreover, the effective transition frequencies correspond roughly to the average frequencies of transitions with favorable Franck-Condon factor.

B. Rovibrational ground state of $X^1\Sigma_g^+$

A similar fit can be performed for the dynamical polarizability of $X^1\Sigma_g^+$ molecules in the ($v_X = 0, N = 0$) level [Fig. 8(b)]. Frequency domains from $\omega/(2\pi c) = 9432 \text{ cm}^{-1}$ to 9960 cm^{-1} , from 10613 cm^{-1} to 12890 cm^{-1} and above 14736 cm^{-1} , corresponding to resonances towards the $b^3\Pi_u$, $A^1\Sigma_u^+$ and $B^1\Pi_u$ excited states, respectively, were excluded from the fit. We omitted to account for levels of the $b^3\Pi_u$ state as they have a very small singlet character. Then, the fit to the numerically calculated dynamical polarizability yields $\omega_\Sigma/(2\pi c) = 11450.31 \text{ cm}^{-1}$, $d_\Sigma = 2.647731 \text{ a.u.}$, $\omega_\Pi/(2\pi c) = 15019.57 \text{ cm}^{-1}$ and $d_\Pi = 2.965774 \text{ a.u.}$ Again, we point out that the effective transition dipole moments obtained are very close to the electronic transition dipole moments taken at equilibrium distance multiplied by the Hönl-London factors, i.e., 2.613 a.u. and 2.959 a.u., respectively. Here, the rRMS of the fit is 0.5%.

C. Excited vibrational states

Both the frequency domain with good Franck-Condon factors and transition dipole moments depend significantly on the initial vibrational level. This is reflected in the variation of the effective parameters when we perform an individual fit for each vibrational level (with $N = 0$) of the $a^3\Sigma_u^+$ ($v_a = 0$ to 40) and $X^1\Sigma_g^+$ ($v_X = 0$ to 124) states. The corresponding parameters, which can be used to reproduce the dynamical polarizabilities in the nonresonant frequency domains, are reported in the Supplemental Material [20]. Figure 9 shows the resulting rRMS values as a function of the vibrational level with respect to the lowest triplet and singlet state.

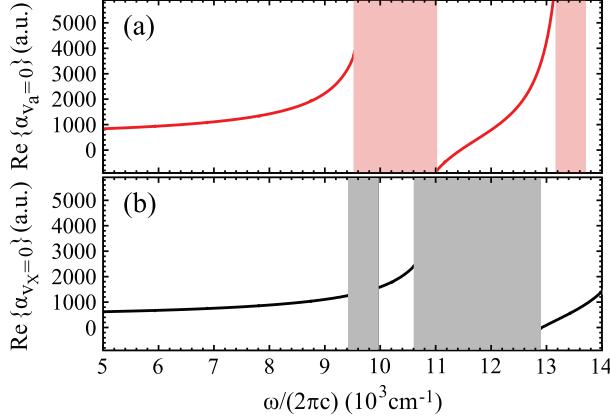


FIG. 8. (Color online) Analytical fits of the dynamical polarizabilities of the $a^3\Sigma_u^+$ molecule in $v_a = 0, N = 0$ (a), and of the $X^1\Sigma_g^+$ molecule in $v_X = 0, N = 0$ (b). Frequency ranges excluded from the fits are indicated as shaded areas. At the scale of the figure, the original curves and the fitted curves are indistinguishable.

Using the ansatz of Eq. (8) gives a poor result for most excited vibrational levels of the $a^3\Sigma_u^+$ potential with an rRMS exceeding 4% in the range of $v_a = 2$ to 27. This behavior is related to the fact that Franck-Condon factors mainly depend on the amplitude of the excited wave function around both the inner and the outer classical turning points of the initial vibrational level studied. The shape of the $a^3\Sigma_u^+$ potential is quite different compared to the relevant excited states. Consequently, the inner turning point region of a given vibrational level v_a will induce couplings to levels of excited molecular states with energies strongly different from those related to couplings induced by the outer turning point region. This effect mainly occurs for the excited $^3\Sigma_g^+$ potential wells as they are deep. Instead, the depth of the $^3\Pi_g$ potential is not sufficient to create such a variation.

Thus we added one more transition term to the ansatz of Eq. (8) in order to account for both the inner and outer part of the $a^3\Sigma_u^+$ - $^3\Sigma_g^+$ transitions in the model. This reduced significantly the rRMS of the effective polarizabilities of the v_a levels (see Fig. 9). We want to emphasize that such an interpretation gives a reasonable physical picture for most levels. However, for some levels like the deeply bound ones or those close to the dissociation limits, the three-effective-transition model is somewhat artificial and the effective parameters should be taken only as numerical parameters needed to easily obtain the corresponding polarizability.

IX. CONCLUSION

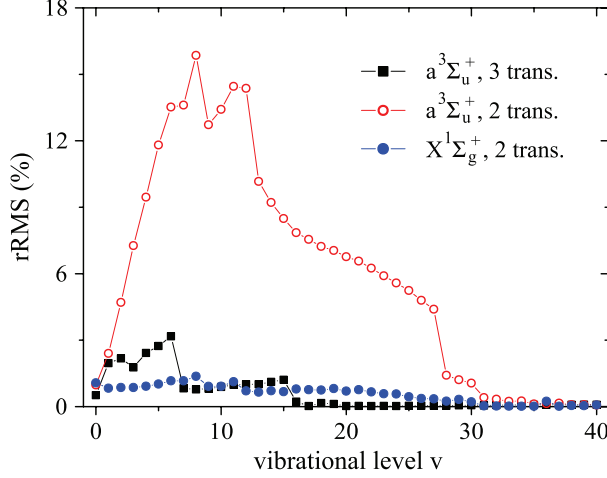


FIG. 9. (Color online) Relative root mean square (rRMS) values of the analytical fits to the numerically calculated dynamical polarizabilities. Blue closed (red open) circles correspond to fit results obtained with the "two-effective-transitions" ansatz for the vibrational levels v_a of $a^3\Sigma_u^+$ (v_X of $X^1\Sigma_g^+$), whereas the black closed squares stem from fits including a third effective transition to represent the dynamical polarizabilities with respect to v_a , which significantly increases the accuracy (see text). The rRMS values for $v_X > 40$ do not exceed 0.1% (not shown here).

We have studied the dynamical polarizability of the $^{87}\text{Rb}_2$ molecule in the rovibrational ground state of the $a^3\Sigma_u^+$ potential. Calculations of both, the real and imaginary part are provided and we measured $\text{Re}\{\alpha(\omega)\}$ at $\lambda = 1064.5 \text{ nm}$. Our experimental and theoretical findings show good agreement. From our computed value of $\text{Im}\{\alpha(\omega)\}$ at this wavelength, we expect trapping times of the molecules on the order of seconds for lattice depths around $50 E_R$, which was confirmed by our observations. We also have investigated theoretically the dynamical polarizability of the singlet ground state $X^1\Sigma_g^+$. These results are interesting for future STIRAP transfer of Rb_2 to the corresponding rovibronic ground state. Furthermore, we have introduced a simple analytical expression to parametrize the dynamical polarizabilities for all levels of both, $a^3\Sigma_u^+$ and $X^1\Sigma_g^+$ states. By fitting this expression to the numerical results, we have extracted effective parameters, which can be used to reproduce $\text{Re}\{\alpha(\omega)\}$ of a given vibrational state with high fidelity. The precise knowledge of the dynamical polarizability enables accurate control of optical dipole potentials and therefore is of importance for future experiments with deeply bound Rb_2 molecules.

X. Appendix

A. Polarizability of the Rb⁺ core.

As the two ionic Rb⁺ cores are only weakly perturbing each other, we consider the molecular core polarizability as twice the atomic Rb⁺ polarizability. First, we calculate the atomic polarizabilities at imaginary frequencies $\alpha_{Rb}(i\omega)$ [50], which includes only the contribution of the valence electron. We subtract them from the values of Ref. [23], where the resulting differences represent the contribution of the core electrons, and thus the Rb⁺ polarizability. Following Ref. [23] this estimate assumes that the influence of the valence electrons on the core polarizability is negligible.

We use an ansatz similar to the one of Eq. (8) to model the core polarizability with two effective transitions. This yields the effective frequencies $\omega/(2\pi c) = 165912 \text{ cm}^{-1}$ and 362918 cm^{-1} , and the effective dipole moments 2.72799 a.u. and 1.40119 a.u. We note that these two transition frequencies are on the order of magnitude of the main transition in Rb⁺ and Rb²⁺, respectively. The core polarizability is a small contribution slowly varying from 17.9 a.u. at vanishing frequency up to 18.1 a.u. in the optical domain relevant here.

B. Transition electric dipole moments.

For the sake of completeness we show in Figure 10 the transition electric dipole moments included in the calculations of the dynamical polarizabilities as functions of the internuclear distances. The corresponding numerical values are given in the Supplemental Material [20]. Some of the data with respect to the lowest transitions have already been reported in Refs. [25, 26]. The largest TEDMs in the range of the PECs concern the first excited Σ^+ and Π potentials [see Fig. 10(a)]. At large distances the molecular excited electronic wave functions become close to the form $[\phi_{5s}(1)\phi_{nl}(2) \pm \phi_{5s}(2)\phi_{nl}(1)]/\sqrt{2}$ and therefore the TEDMs converge towards d_{5s-nl} , which is equal to the atomic TEDMs multiplied by $\sqrt{2}$. We find $d_{5s-5p} = 4.23$ a.u. and $d_{5s-6p} = 0.347$ a.u., in excellent agreement with the values extracted from the NIST database [40] (4.226 a.u. and 0.3531 a.u.), obtained by averaging the TEDMs corresponding to $5s - np_{1/2}$ and $5s - np_{3/2}$ for $n = 5$ and 6, respectively. This confirms the good quality of the present representations of the atomic electronic wave functions.

XI. Acknowledgements

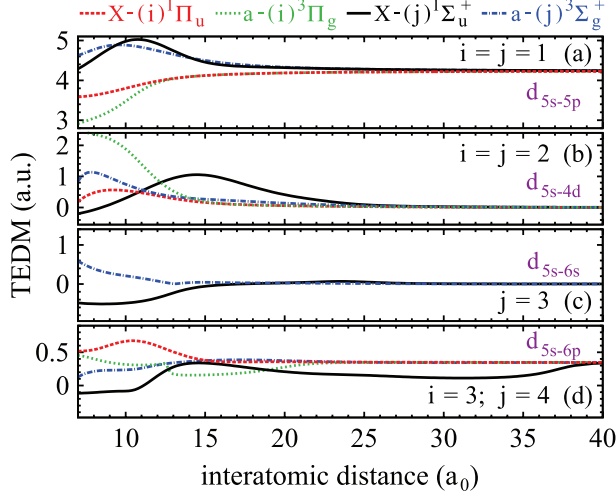


FIG. 10. (Color online) Computed transition electric dipole moments (TEDMs) for the main transitions from the $a^3\Sigma_u^+$ and the $X^1\Sigma_g^+$ states to the states correlated to the $5s + 5p$ dissociation limit (a), the $5s + 4d$ dissociation limit (b), the $5s + 6s$ dissociation limit (c), and the $5s + 6p$ dissociation limit (d). The individual curves can be assigned to the corresponding transitions as indicated on top of the graph using the numbers i and j . At large distances the TEDMs converge towards d_{5s-nl} which is equal to the atomic TEDMs multiplied by $\sqrt{2}$ (see text).

This work was funded by the German Research Foundation (DFG). R.V. acknowledges partial support from Agence Nationale de la Recherche (ANR), under the project COPOMOL (contract ANR-13-IS04-0004-01).

- [1] R. V. Krems, Phys. Chem. Chem. Phys. **10**, 4079 (2008).
- [2] L. D. Carr, D. DeMille, R. V. Krems, and J. Ye, New J. Phys. **11**, 055049 (2009).
- [3] D. Jaksch, V. Venturi, J. I. Cirac, C. J. Williams, and P. Zoller, Phys. Rev. Lett. **89**, 040402 (2002).
- [4] V. V. Flambaum and M. G. Kozlov, Phys. Rev. Lett. **99**, 150801 (2007).
- [5] D. DeMille, S. Sainis, J. Sage, T. Bergeman, S. Kotochigova, and E. Tiesinga, Phys. Rev. Lett. **100**, 043202 (2008).
- [6] T. Zelevinsky, S. Kotochigova, and J. Ye, Phys. Rev. Lett. **100**, 043201 (2008).
- [7] C. Chin, V. V. Flambaum, and M. G. Kozlov, New J. Phys. **11**, 055048 (2009).
- [8] D. DeMille, Phys. Rev. Lett. **88**, 067901 (2002).
- [9] D. Yelin, K. Kirby, and R. Côté, Phys. Rev. A **74**, 050301(R) (2006).

- [10] A. Micheli, G. K. Brennen, and P. Zoller, Nat. Phys. **2**, 341 (2006).
- [11] K.-K. Ni, S. Ospelkaus, M. H. G. de Miranda, A. Pe'er, B. Neyenhuis, J. J. Zirbel, S. Kotochigova, P. S. Julienne, D. S. Jin, and J. Ye, Science **322**, 231 (2008).
- [12] F. Lang, K. Winkler, C. Strauss, R. Grimm, and J. Hecker Denschlag, Phys. Rev. Lett. **101**, 133005 (2008).
- [13] J. G. Danzl, M. J. Mark, E. Haller, M. Gustavsson, R. Hart, J. Aldegunde, J. M. Hutson, and H.-C. Nägerl, Nat. Phys. **6**, 265 (2010).
- [14] T. Takekoshi, L. Reichsöllner, A. Schindewolf, J. M. Hutson, C. Ruth Le Sueur, O. Dulieu, F. Ferlaino, R. Grimm, and H.-C. Nägerl, Phys. Rev. Lett. **113**, 205301 (2014).
- [15] P. K. Molony, P. D. Gregory, Z. Ji, B. Lu, M. P. Köppinger, C. Ruth Le Sueur, C. L. Blackley, J. M. Hutson, and S. L. Cornish, Phys. Rev. Lett. **113**, 255301 (2014).
- [16] B. Yan, S. A. Moses, B. Gadway, J. P. Covey, K. R. A. Hazzard, A. M. Rey, D. S. Jin, and J. Ye, Nature **501**, 521 (2013).
- [17] B. Zhu, B. Gadway, M. Foss-Feig, J. Schachenmayer, M. L. Wall, K. R. A. Hazzard, B. Yan, S. A. Moses, J. P. Covey, D. S. Jin, J. Ye, M. Holland, and A. M. Rey, Phys. Rev. Lett. **112**, 070404 (2014).
- [18] B. Drews *et al.* (in preparation).
- [19] R. Vexiau, N. Bouloufa, M. Aymar, J. G. Danzl, M. J. Mark, H.-C. Nägerl, and O. Dulieu, Eur. Phys. J. D **65**, 243 (2011).
- [20] See Supplemental Material at [URL] for the results of the analytical fits to the calculated polarizabilities corresponding to different vibrational levels v_a (v_X) of $a^3\Sigma_u^+$ ($X^1\Sigma_g^+$) using two or three effective transitions and for the numerical values of the transition electric dipole moments starting from either the lowest triplet state ($a^3\Sigma_u^+$) or singlet state ($X^1\Sigma_g^+$) towards the most relevant excited potentials.
- [21] M. Deiß, B. Drews, B. Deissler, and J. Hecker Denschlag, Phys. Rev. Lett. **113**, 233004 (2014).
- [22] R. Grimm, M. Weidemüller, and Y. B. Ovchinnikov, Adv. At. Mol. Opt. Phys. **42**, 95 (2000).
- [23] A. Derevianko, S. G. Porsev, and J. F. Babb, At. Data Nucl. Data Tables **96**, 323 (2010).
- [24] Y. Guan, X. Han, J. Yang, Z. Zhou, X. Dai, E. H. Ahmed, A. M. Lyyra, S. Magnier, V. S. Ivanov, A. S. Skublov, and V. B. Sovkov, J. Chem. Phys. **139**, 144303 (2013).
- [25] R. Beuc, M. Movre, V. Horvatic, C. Vadla, O. Dulieu, and M. Aymar, Phys. Rev. A **75**, 032512 (2007).
- [26] J. Lozeille, A. Fioretti, C. Gabbanini, Y. Huang, H. K. Pechkis, D. Wang, P. L. Gould, E. E. Eyler, W. C. Stwalley, M. Aymar, and O. Dulieu, Eur. Phys. J. D **39**, 261 (2006).
- [27] M. Aymar and O. Dulieu, J. Chem. Phys. **122**, 204302 (2005).

- [28] M. Foucraut, P. Millie, and J. P. Daudey, *J. Chem. Phys.* **96**, 1257 (1992).
- [29] W. Müller, J. Flesch, and W. Meyer, *J. Chem. Phys.* **80**, 3297 (1984).
- [30] M. Aymar and O. Dulieu, *J. Chem. Phys.* **125**, 047101 (2006).
- [31] T. Takekoshi, C. Strauss, F. Lang, J. Hecker Denschlag, M. Lysebo, L. Veseth, *Phys. Rev. A* **83**, 062504 (2011).
- [32] M. A. Bellos, D. Rahmlow, R. Carollo, J. Banerjee, O. Dulieu, A. Gerdes, E. E. Eyler, P. L. Gould, and W. C. Stwalley, *Phys. Chem. Chem. Phys.* **13**, 18880 (2011).
- [33] O. Dulieu and P. S. Julienne, *J. Chem. Phys.* **103**, 60 (1995).
- [34] V. Kokouoline, O. Dulieu, R. Kosloff, and F. Masnou-Seeuws, *J. Chem. Phys.* **110**, 9865 (1999).
- [35] G. Thalhammer, K. Winkler, F. Lang, S. Schmid, R. Grimm, and J. Hecker Denschlag, *Phys. Rev. Lett.* **96**, 050402 (2006).
- [36] S. Friebel, C. D'Andrea, J. Walz, M. Weitz, and T. W. Hänsch, *Phys. Rev. A* **57**, R20(R) (1998).
- [37] J. Hecker Denschlag, H. Häffner, C. McKenzie, A. Browaeys, D. Cho, C. Helmerson, S. Rolston, and W. D. Phillips, *J. Phys. B: At. Mol. Opt. Phys.* **35**, 3095 (2002).
- [38] R. Jáuregui, N. Poli, G. Roati, and G. Modugno, *Phys. Rev. A* **64**, 033403 (2001).
- [39] M. Greiner, *Ultracold quantum gases in three-dimensional optical lattice potentials*, PhD thesis, Ludwig-Maximilians-Universität München (2003).
- [40] J. E. Sansonetti, W. C. Martin, and S. L. Young, *Handbook of Basic Atomic Spectroscopic Data* (version 1.1.3), National Institute of Standards and Technology, Gaithersburg, MD (2005). Available at <http://physics.nist.gov/Handbook>.
- [41] M. S. Safranova, C. J. Williams, and C. W. Clark, *Phys. Rev. A* **67**, 040303(R) (1999).
- [42] M. S. Safranova, C. J. Williams, and C. W. Clark, *Phys. Rev. A* **69**, 022509 (2004).
- [43] M. Tomza and R. Moszyński (private communication). The given value is calculated using the method described in [44].
- [44] M. Tomza, W. Skomorowski, M. Musiał, R. González-Férez, C. P. Koch, and R. Moszynski, *Mol. Phys.* **111**, 1781 (2013).
- [45] A. Derevianko, W. R. Johnson, M. S. Safranova, and J. F. Babb, *Phys. Rev. Lett.* **82**, 3589 (1999).
- [46] J. Deiglmayr, M. Aymar, R. Wester, M. Weidemüller, and O. Dulieu, *J. Chem. Phys.* **129**, 064309 (2008).
- [47] T. Rom, T. Best, O. Mandel, A. Widera, M. Greiner, T. W. Hänsch, and I. Bloch, *Phys. Rev. Lett.* **93**, 073002 (2004).

- [48] C. Strauss, T. Takekoshi, F. Lang, K. Winkler, R. Grimm, J. Hecker Denschlag, and E. Tiemann, Phys. Rev. A **82**, 052514 (2010).
- [49] A. N. Drozdova, A. V. Stolyarov, M. Tamanis, R. Ferber, P. Crozet, and A. J. Ross, Phys. Rev. A **88**, 022504 (2013).
- [50] M. Lepers, R. Vexiau, M. Aymar, N. Bouloufa-Maafa, and O. Dulieu, Phys. Rev. A **88**, 032709 (2013).

Supplemental Material

Transition electric dipole moment (in a.u.) starting from the Rb_2 ground state (singlet Sigma_g^+) towards the 7 lowest singlet Pi_u states (labelled as (1) to (7)), as functions of the internuclear distance R (in a.u.).

#R	(1)	(2)	(3)	(4)	(5)	(6)	(7)
3	11.986	30.677	-0.8479	-0.0108	-0.0622	-0.3092	-0.7384
3.2	12.710	31.592	-0.4008	-0.3098	-0.261	-0.4221	-0.3179
3.6	15.366	31.422	-0.2913	-0.3361	-0.0716	-0.1565	-0.4413
3.8	17.770	30.516	-0.3394	-0.0624	-0.0738	-0.4676	-0.0951
6.8	35.790	0.0986	0.5169	-0.0795	-0.0022	-0.1551	-0.1965
7	35.838	0.1887	0.5171	-0.0615	0.0238	-0.1627	-0.188
7.2	35.896	0.2669	0.5179	-0.0431	0.0502	-0.1675	-0.1773
7.4	35.967	0.3339	0.5201	-0.0247	0.0761	-0.1674	-0.1669
7.6	36.052	0.3903	0.5241	-0.0069	0.1006	-0.1614	-0.1584
7.8	36.153	0.4371	0.5304	0.0099	0.1228	-0.1502	-0.1523
8	36.269	0.475	0.539	0.0252	0.1419	-0.1349	-0.1482
8.2	36.400	0.5051	0.5497	0.0388	0.157	-0.1166	-0.1453
8.4	36.544	0.5282	0.5624	0.0505	0.1677	-0.0969	-0.1433
8.6	36.700	0.545	0.5764	0.0602	0.1738	-0.0768	-0.1414
8.8	36.866	0.5563	0.5914	0.0677	0.1754	-0.0576	-0.1394
9	37.041	0.5627	0.6066	0.0731	0.1729	-0.04	-0.1369
9.4	37.413	0.5636	0.6354	0.0774	0.1575	-0.0109	-0.1293
9.6	37.606	0.5592	0.6478	0.0764	0.1456	0.0003	-0.1237
9.8	37.803	0.5521	0.6582	0.0734	0.1315	0.0094	-0.1164
10	38.001	0.5428	0.6662	0.0684	0.1158	0.0166	-0.1068
10.2	38.200	0.5315	0.6714	0.0616	0.099	0.0221	-0.0942
10.4	38.398	0.5187	0.6736	0.0531	0.0817	0.0261	-0.0775
10.6	38.595	0.5045	0.6728	0.043	0.0643	0.0289	-0.0564
10.8	38.788	0.489	0.669	0.0315	0.0474	0.0307	-0.0324
11	38.977	0.4725	0.6623	0.0188	0.0316	0.0317	-0.0089
11.2	39.161	0.4552	0.6529	0.0051	0.0173	0.0322	0.0105
11.4	39.338	0.4372	0.6411	-0.0093	0.0049	0.0323	0.0245
11.6	39.509	0.4186	0.6274	-0.0242	-0.0052	0.0322	0.0338
11.8	39.672	0.3997	0.6119	-0.0393	-0.0129	0.0323	0.0394
12	39.827	0.3807	0.5953	-0.0543	-0.0181	0.0327	0.0422
12.2	39.973	0.3616	0.5777	-0.0689	-0.0208	0.0339	0.0427
12.4	40.110	0.3428	0.5597	-0.0828	-0.0215	0.0365	0.0408
12.6	40.238	0.3244	0.5415	-0.0957	-0.0205	0.042	0.0349
12.8	40.358	0.3064	0.5234	-0.1074	-0.0182	0.0528	0.0142
13	40.469	0.2891	0.5057	-0.118	-0.0152	0.052	-0.0201
13.8	40.835	0.2279	0.4427	-0.1486	-0.0019	0.0357	-0.0697
14	40.910	0.2148	0.4294	-0.1537	0.0008	0.0332	-0.0774
14.2	40.979	0.2025	0.4173	-0.1579	0.0032	0.0311	-0.082
14.4	41.043	0.1911	0.4064	-0.1611	0.0052	0.0293	-0.084
14.6	41.102	0.1804	0.3966	-0.1635	0.0069	0.0279	-0.084
14.8	41.157	0.1706	0.388	-0.165	0.0083	0.0267	-0.0826
15	41.208	0.1614	0.3806	-0.1657	0.0095	0.0257	-0.0803
15.2	41.256	0.153	0.3742	-0.1656	0.0106	0.0251	-0.0775
15.4	41.300	0.1451	0.3689	-0.1646	0.0115	0.0246	-0.0742
15.6	41.341	0.1379	0.3646	-0.1627	0.0123	0.0243	-0.0707

15.8	41.380	0.1312	0.3612	-0.1601	0.013	0.0241	-0.0671
16	41.416	0.125	0.3586	-0.1567	0.0138	0.0241	-0.0635
16.2	41.450	0.1193	0.3567	-0.1527	0.0145	0.0241	-0.06
16.4	41.483	0.114	0.3555	-0.1479	0.0152	0.0242	-0.0565
16.6	41.513	0.1091	0.3547	-0.1426	0.016	0.0244	-0.0532
16.8	41.542	0.1045	0.3544	-0.1369	0.0168	0.0246	-0.05
17	41.569	0.1003	0.3544	-0.1307	0.0176	0.0248	-0.047
17.2	41.595	0.0964	0.3546	-0.1243	0.0185	0.025	-0.0442
17.4	41.620	0.0927	0.3549	-0.1177	0.0194	0.0252	-0.0415
17.6	41.643	0.0893	0.3553	-0.1111	0.0203	0.0254	-0.039
17.8	41.665	0.0861	0.3558	-0.1046	0.0212	0.0256	-0.0367
18	41.687	0.0831	0.3562	-0.0981	0.0222	0.0257	-0.0345
18.2	41.707	0.0803	0.3565	-0.0918	0.0231	0.0258	-0.0324
18.4	41.726	0.0776	0.3568	-0.0858	0.0241	0.0259	-0.0305
18.6	41.745	0.0751	0.357	-0.08	0.0252	0.026	-0.0287
18.8	41.763	0.0728	0.3572	-0.0745	0.0262	0.026	-0.0269
19	41.780	0.0705	0.3573	-0.0693	0.0273	0.026	-0.0253
19.2	41.796	0.0684	0.3573	-0.0644	0.0284	0.026	-0.0237
19.4	41.812	0.0663	0.3573	-0.0596	0.0296	0.026	-0.0222
19.8	41.841	0.0625	0.357	-0.0508	0.032	0.0259	-0.0194
20	41.855	0.0606	0.3569	-0.0466	0.0332	0.0259	-0.0181
20.2	41.868	0.0589	0.3567	-0.0424	0.0344	0.026	-0.0168
20.4	41.881	0.0572	0.3565	-0.0384	0.0355	0.026	-0.0155
20.8	41.905	0.054	0.356	-0.0304	0.0376	0.0261	-0.0131
21	41.916	0.0524	0.3558	-0.0265	0.0384	0.0262	-0.012
21.2	41.927	0.0509	0.3555	-0.0227	0.0389	0.0264	-0.0109
21.4	41.938	0.0495	0.3553	-0.0192	0.0392	0.0265	-0.0098
21.6	41.948	0.0481	0.3551	-0.0158	0.0393	0.0267	-0.0087
21.8	41.958	0.0467	0.3548	-0.0128	0.0391	0.027	-0.0077
22	41.967	0.0454	0.3546	-0.0101	0.0387	0.0272	-0.0067
22.4	41.985	0.0428	0.3541	-0.0057	0.0375	0.0277	-0.0048
22.6	41.994	0.0416	0.3539	-0.004	0.0368	0.028	-0.0039
22.8	42.002	0.0404	0.3537	-0.0025	0.036	0.0283	-0.003
23	42.010	0.0392	0.3535	-0.0013	0.0352	0.0286	-0.0021
23.4	42.025	0.037	0.3531	0.0006	0.0335	0.0293	-0.0004
23.6	42.033	0.0359	0.3529	0.0013	0.0327	0.0296	0.0004
23.8	42.040	0.0349	0.3527	0.0019	0.0319	0.0299	0.0011
24	42.046	0.0339	0.3526	0.0023	0.0311	0.0302	0.0019
24.2	42.053	0.0329	0.3524	0.0027	0.0303	0.0305	0.0026
24.4	42.059	0.0319	0.3522	0.003	0.0295	0.0308	0.0033
24.6	42.065	0.031	0.3521	0.0032	0.0288	0.031	0.004
24.8	42.071	0.0301	0.352	0.0034	0.028	0.0313	0.0047
25	42.077	0.0292	0.3518	0.0035	0.0273	0.0315	0.0053
25.2	42.083	0.0284	0.3517	0.0036	0.0266	0.0317	0.0059
25.4	42.088	0.0275	0.3516	0.0036	0.0259	0.0319	0.0065
25.6	42.093	0.0267	0.3514	0.0036	0.0252	0.0321	0.0071
25.8	42.099	0.026	0.3513	0.0036	0.0245	0.0323	0.0077
26	42.103	0.0252	0.3512	0.0036	0.0238	0.0324	0.0082
26.2	42.108	0.0244	0.3511	0.0035	0.0231	0.0326	0.0087
26.4	42.113	0.0237	0.351	0.0034	0.0225	0.0327	0.0092

26.6	42.117	0.023	0.3509	0.0034	0.0218	0.0328	0.0097
26.8	42.122	0.0223	0.3508	0.0033	0.0212	0.0328	0.0101
27	42.126	0.0216	0.3507	0.0032	0.0205	0.0329	0.0105
27.2	42.130	0.021	0.3506	0.003	0.0199	0.0329	0.0109
27.4	42.134	0.0203	0.3505	0.0029	0.0192	0.0329	0.0113
27.6	42.138	0.0197	0.3504	0.0028	0.0186	0.0329	0.0117
27.8	42.142	0.0191	0.3504	0.0027	0.018	0.0329	0.012
28	42.146	0.0185	0.3503	0.0026	0.0174	0.0329	0.0123
28.2	42.149	0.0179	0.3502	0.0025	0.0168	0.0328	0.0126
28.4	42.153	0.0174	0.3501	0.0023	0.0162	0.0328	0.0128
28.6	42.156	0.0168	0.35	0.0022	0.0156	0.0327	0.0131
28.8	42.160	0.0163	0.35	0.0021	0.015	0.0326	0.0133
29	42.163	0.0157	0.3499	0.002	0.0144	0.0325	0.0135
29.2	42.166	0.0152	0.3498	0.0019	0.0139	0.0324	0.0137
29.4	42.169	0.0147	0.3498	0.0018	0.0133	0.0322	0.0139
29.6	42.172	0.0142	0.3497	0.0017	0.0128	0.0321	0.014
29.8	42.175	0.0138	0.3496	0.0016	0.0122	0.032	0.0142
30	42.178	0.0133	0.3496	0.0015	0.0117	0.0318	0.0143
30.2	42.180	0.0128	0.3495	0.0014	0.0112	0.0316	0.0145
30.4	42.183	0.0124	0.3494	0.0013	0.0107	0.0315	0.0146
30.6	42.186	0.012	0.3494	0.0012	0.0102	0.0313	0.0147
30.8	42.188	0.0116	0.3493	0.0011	0.0097	0.0311	0.0148
31	42.191	0.0112	0.3493	0.001	0.0092	0.0309	0.0149
31.2	42.193	0.0108	0.3492	0.0009	0.0087	0.0307	0.015
31.4	42.195	0.0104	0.3492	0.0009	0.0083	0.0305	0.0151
31.6	42.198	0.0101	0.3491	0.0008	0.0078	0.0302	0.0151
31.8	42.200	0.0097	0.3491	0.0007	0.0074	0.03	0.0152
32	42.202	0.0094	0.349	0.0007	0.007	0.0298	0.0153
32.2	42.204	0.0091	0.3489	0.0006	0.0066	0.0295	0.0153
32.4	42.206	0.0087	0.3489	0.0005	0.0062	0.0293	0.0153
32.6	42.208	0.0084	0.3489	0.0005	0.0058	0.0291	0.0154
32.8	42.210	0.0081	0.3488	0.0004	0.0055	0.0288	0.0154
33	42.212	0.0079	0.3488	0.0004	0.0052	0.0285	0.0154
33.2	42.214	0.0076	0.3487	0.0004	0.0048	0.0283	0.0155
33.4	42.216	0.0073	0.3487	0.0003	0.0045	0.028	0.0155
33.6	42.218	0.0071	0.3486	0.0003	0.0042	0.0277	0.0155
33.8	42.219	0.0068	0.3486	0.0003	0.0039	0.0275	0.0155
34	42.221	0.0066	0.3485	0.0002	0.0037	0.0272	0.0155
34.2	42.223	0.0064	0.3485	0.0002	0.0034	0.0269	0.0155
34.4	42.224	0.0062	0.3485	0.0002	0.0032	0.0266	0.0155
34.6	42.226	0.006	0.3484	0.0001	0.0029	0.0263	0.0155
34.8	42.227	0.0058	0.3484	0.0001	0.0027	0.0261	0.0155
35	42.229	0.0056	0.3484	0.0001	0.0025	0.0258	0.0155
35.2	42.230	0.0054	0.3483	0.0001	0.0023	0.0255	0.0155
35.4	42.232	0.0052	0.3483	0.0001	0.0021	0.0252	0.0155
35.6	42.233	0.005	0.3483	0	0.002	0.0249	0.0155
35.8	42.235	0.0049	0.3482	0	0.0018	0.0246	0.0154
36	42.236	0.0047	0.3482	0	0.0016	0.0242	0.0154
36.2	42.237	0.0046	0.3482	0	0.0015	0.0239	0.0154
36.4	42.239	0.0044	0.3481	0	0.0014	0.0236	0.0154

36.6	42.240	0.0043	0.3481	0	0.0012	0.0233	0.0154
36.8	42.241	0.0042	0.3481	0	0.0011	0.023	0.0154
37	42.242	0.004	0.3481	0	0.001	0.0227	0.0153
37.2	42.243	0.0039	0.348	0	0.0009	0.0223	0.0153
37.4	42.245	0.0038	0.348	0	0.0008	0.022	0.0153
37.6	42.246	0.0037	0.348	0	0.0007	0.0217	0.0153
37.8	42.247	0.0036	0.348	0	0.0007	0.0213	0.0152
38	42.248	0.0035	0.3479	0	0.0006	0.021	0.0152
38.2	42.249	0.0034	0.3479	0.0001	0.0005	0.0206	0.0152
39.4	42.255	0.0028	0.3478	0.0001	0.0002	0.0185	0.015
39.6	42.256	0.0027	0.3478	0.0001	0.0002	0.0182	0.015
39.8	42.257	0.0027	0.3478	0.0001	0.0001	0.0178	0.0149
40	42.258	0.0026	0.3478	0.0001	0.0001	0.0174	0.0149

Transition electric dipole moment (in a.u.) starting from the Rb_2 lowest triplet Sigma_u^+ state towards the 9 lowest triplet Pi_g states (labelled as (1) to (9)), as functions of the internuclear distance R (in a.u.).

#	R	(1)	(2)	(3)	(4)	(5)	(6)	(7)	(8)	(9)
5.20000	2.55750	2.73160	0.48350	-0.44970	0.23470	0.07920	-0.07260	0.12370	-0.01190	
5.40000	2.59450	2.70830	0.46690	-0.37530	0.32370	0.09640	-0.06980	0.10840	-0.03800	
5.60000	2.63860	2.67590	0.45960	-0.29750	0.36890	0.11550	-0.06600	0.09340	-0.06010	
5.80000	2.68520	2.63890	0.45780	-0.24780	0.36860	0.13850	-0.06260	0.08020	-0.07670	
6.00000	2.73090	2.60120	0.45880	-0.22100	0.33880	0.17230	-0.05970	0.06910	-0.08950	
6.60000	2.84850	2.50390	0.46150	-0.19410	0.09040	0.29120	-0.05080	0.03830	-0.12040	
6.80000	2.88090	2.47880	0.45900	-0.19030	-0.12210	0.25200	-0.04490	0.02710	-0.13140	
7.00000	2.91070	2.45670	0.45410	-0.18640	-0.13990	0.21640	-0.03610	0.01630	-0.14420	
7.20000	2.93890	2.43690	0.44680	-0.18200	-0.15210	0.18390	-0.02450	0.00680	-0.15970	
7.40000	2.96600	2.41840	0.43740	-0.17670	-0.16130	0.15420	-0.01020	0.00040	-0.17760	
7.60000	2.99300	2.40030	0.42630	-0.17060	-0.16870	0.12720	0.00610	0.00470	-0.19330	
8.20000	3.07880	2.33820	0.38900	-0.14700	-0.18630	0.06220	0.06000	0.00080	-0.19480	
8.40000	3.11100	2.31170	0.37700	-0.13730	-0.19180	0.04570	0.07770	-0.00720	-0.18780	
8.60000	3.14590	2.28080	0.36580	-0.12660	-0.19730	0.03200	0.09470	-0.01420	-0.17910	
8.80000	3.18370	2.24480	0.35570	-0.11470	-0.20310	0.02100	0.11040	-0.02020	-0.16890	
9.00000	3.22470	2.20270	0.34680	-0.10160	-0.20910	0.01290	0.12450	-0.02390	-0.15770	
9.40000	3.31660	2.09790	0.33210	-0.07050	-0.22130	0.00590	0.14640	-0.02290	-0.13530	
9.60000	3.36720	2.03410	0.32640	-0.05240	-0.22680	-0.00690	0.15390	-0.01890	-0.12490	
9.80000	3.42040	1.96230	0.32150	-0.03270	-0.23130	-0.01060	0.15910	-0.01350	-0.11540	
10.00000	3.47560	1.88260	0.31750	-0.01200	-0.23410	-0.01650	0.16220	-0.00750	-0.10670	
10.20000	3.53180	1.79540	0.31430	0.00870	-0.23490	-0.02400	0.16340	-0.00120	-0.09840	
10.40000	3.58810	1.70150	0.31190	0.02840	-0.23380	-0.03220	0.16290	0.00500	-0.09040	
10.60000	3.64350	1.60210	0.31010	0.04600	-0.23120	-0.04060	0.16080	0.01100	-0.08230	
10.80000	3.69690	1.49860	0.30900	0.06110	-0.22780	-0.04880	0.15720	0.01660	-0.07440	
11.00000	3.74730	1.39280	0.30850	0.07340	-0.22400	-0.05650	0.15210	0.02180	-0.06690	
11.20000	3.79410	1.28670	0.30860	0.08310	-0.22040	-0.06360	0.14520	0.02670	-0.06010	
11.40000	3.83680	1.18200	0.30950	0.09020	-0.21720	-0.07030	0.13660	0.03110	-0.05420	
11.60000	3.87520	1.08040	0.31110	0.09480	-0.21460	-0.07660	0.12580	0.03510	-0.04930	
11.80000	3.90920	0.98320	0.31360	0.09660	-0.21240	-0.08260	0.11240	0.03880	-0.04530	
12.00000	3.93910	0.89150	0.31740	0.09430	-0.21060	-0.08840	0.09580	0.04190	-0.04210	
12.20000	3.96510	0.80600	0.32370	0.08350	-0.20890	-0.09320	0.07530	0.04470	-0.03950	
12.40000	3.98780	0.72710	0.33490	0.04250	-0.20710	-0.09530	0.05100	0.04690	-0.03760	
12.60000	4.00740	0.65470	0.29730	0.16680	-0.20470	-0.09210	0.02520	0.04880	-0.03600	
12.80000	4.02440	0.58890	0.19880	0.28120	-0.20150	-0.08260	0.00260	0.05020	-0.03500	
13.00000	4.03930	0.52940	0.17360	0.30160	-0.19710	-0.06850	-0.01400	0.05130	-0.03440	
13.20000	4.05220	0.47590	0.16430	0.31090	-0.19120	-0.05280	-0.02480	0.05230	-0.03430	
13.40000	4.06360	0.42790	0.16000	0.31710	-0.18380	-0.03710	-0.03100	0.05330	-0.03490	
13.60000	4.07370	0.38500	0.15790	0.32220	-0.17490	-0.02250	-0.03350	0.05460	-0.03630	
13.80000	4.08270	0.34670	0.15680	0.32650	-0.16480	-0.00930	-0.03280	0.05600	-0.03910	
14.00000	4.09070	0.31270	0.15630	0.33020	-0.15360	0.00210	-0.02960	0.05680	-0.04360	
14.20000	4.09800	0.28260	0.15630	0.33330	-0.14160	0.01190	-0.02490	0.05530	-0.05050	
14.40000	4.10460	0.25590	0.15670	0.33600	-0.12920	0.02000	-0.02010	0.05080	-0.05870	
14.60000	4.11060	0.23220	0.15730	0.33800	-0.11650	0.02660	-0.01610	0.04460	-0.06630	
14.80000	4.11610	0.21140	0.15810	0.33950	-0.10390	0.03180	-0.01310	0.03920	-0.07170	
15.00000	4.12110	0.19300	0.15920	0.34040	-0.09160	0.03570	-0.01120	0.03560	-0.07520	

15.20000	4.12590	0.17680	0.16050	0.34080	-0.07980	0.03850	-0.01020	0.03350	-0.07770
15.40000	4.13020	0.16260	0.16200	0.34070	-0.06860	0.04040	-0.00970	0.03250	-0.07950
15.60000	4.13430	0.15010	0.16370	0.34010	-0.05810	0.04150	-0.00950	0.03200	-0.08090
15.80000	4.13820	0.13910	0.16570	0.33910	-0.04840	0.04180	-0.00960	0.03200	-0.08210
16.00000	4.14170	0.12940	0.16790	0.33770	-0.03950	0.04170	-0.00990	0.03220	-0.08320
16.20000	4.14510	0.12100	0.17030	0.33590	-0.03140	0.04110	-0.01020	0.03240	-0.08400
16.40000	4.14830	0.11350	0.17300	0.33390	-0.02410	0.04020	-0.01060	0.03280	-0.08470
16.60000	4.15130	0.10700	0.17600	0.33150	-0.01760	0.03900	-0.01110	0.03320	-0.08520
16.80000	4.15420	0.10120	0.17930	0.32880	-0.01180	0.03780	-0.01160	0.03370	-0.08550
17.00000	4.15690	0.09610	0.18280	0.32580	-0.00660	0.03640	-0.01210	0.03410	-0.08550
17.20000	4.15950	0.09150	0.18670	0.32260	-0.00210	0.03500	-0.01250	0.03460	-0.08510
17.40000	4.16190	0.08750	0.19090	0.31900	0.00190	0.03360	-0.01290	0.03510	-0.08400
17.60000	4.16430	0.08390	0.19550	0.31510	0.00540	0.03220	-0.01320	0.03560	-0.08190
17.80000	4.16650	0.08060	0.20050	0.31090	0.00850	0.03080	-0.01340	0.03610	-0.07820
18.00000	4.16860	0.07760	0.20580	0.30620	0.01120	0.02950	-0.01360	0.03660	-0.07210
18.20000	4.17070	0.07500	0.21160	0.30120	0.01350	0.02820	-0.01360	0.03710	-0.06280
18.40000	4.17260	0.07250	0.21770	0.29570	0.01550	0.02700	-0.01350	0.03760	-0.05090
18.60000	4.17450	0.07020	0.22430	0.28970	0.01720	0.02580	-0.01340	0.03820	-0.03880
18.80000	4.17620	0.06810	0.23130	0.28310	0.01860	0.02470	-0.01310	0.03870	-0.02880
19.00000	4.17790	0.06610	0.23860	0.27590	0.01980	0.02370	-0.01270	0.03920	-0.02140
19.20000	4.17960	0.06420	0.24620	0.26810	0.02080	0.02280	-0.01220	0.03970	-0.01620
20.60000	4.18930	0.05320	0.29970	0.19900	0.02380	0.01830	-0.00710	0.04260	0.00680
20.80000	4.19050	0.05180	0.30600	0.18820	0.02380	0.01800	-0.00620	0.04280	0.00730
21.00000	4.19160	0.05050	0.31170	0.17760	0.02370	0.01780	-0.00530	0.04290	0.00810
21.20000	4.19270	0.04920	0.31680	0.16730	0.02360	0.01760	-0.00440	0.04290	0.00920
21.40000	4.19380	0.04790	0.32140	0.15740	0.02350	0.01750	-0.00350	0.04280	0.01050
21.60000	4.19480	0.04660	0.32540	0.14800	0.02330	0.01750	-0.00250	0.04250	0.01190
21.80000	4.19580	0.04540	0.32890	0.13910	0.02310	0.01750	-0.00160	0.04220	0.01350
22.00000	4.19670	0.04420	0.33190	0.13070	0.02280	0.01760	0.00070	0.04170	0.01520
22.40000	4.19850	0.04180	0.33670	0.11560	0.02230	0.01800	0.00110	0.04040	0.01840
22.60000	4.19940	0.04070	0.33860	0.10880	0.02210	0.01820	0.00200	0.03960	0.02000
22.80000	4.20020	0.03960	0.34020	0.10250	0.02180	0.01860	0.00290	0.03880	0.02150
23.00000	4.20100	0.03850	0.34160	0.09660	0.02160	0.01890	0.00380	0.03790	0.02280
23.40000	4.20250	0.03640	0.34380	0.08610	0.02110	0.01970	0.00540	0.03620	0.02510
23.60000	4.20320	0.03540	0.34470	0.08140	0.02100	0.02020	0.00620	0.03530	0.02610
23.80000	4.20390	0.03440	0.34540	0.07690	0.02080	0.02060	0.00700	0.03450	0.02690
24.00000	4.20460	0.03350	0.34610	0.07280	0.02070	0.02110	0.00770	0.03380	0.02770
24.20000	4.20530	0.03250	0.34660	0.06880	0.02060	0.02160	0.00840	0.03300	0.02830
24.40000	4.20590	0.03160	0.34710	0.06510	0.02060	0.02200	0.00910	0.03240	0.02890
24.60000	4.20650	0.03070	0.34750	0.06160	0.02060	0.02250	0.00970	0.03170	0.02950
24.80000	4.20710	0.02990	0.34780	0.05820	0.02070	0.02300	0.01030	0.03110	0.02990
25.00000	4.20770	0.02900	0.34810	0.05500	0.02080	0.02340	0.01090	0.03060	0.03030
25.20000	4.20830	0.02820	0.34830	0.05190	0.02100	0.02380	0.01140	0.03010	0.03070
25.40000	4.20880	0.02740	0.34850	0.04890	0.02120	0.02420	0.01180	0.02970	0.03100
25.60000	4.20930	0.02660	0.34870	0.04590	0.02150	0.02460	0.01220	0.02940	0.03140
25.80000	4.20980	0.02580	0.34890	0.04300	0.02190	0.02490	0.01250	0.02910	0.03160
26.00000	4.21030	0.02510	0.34900	0.04020	0.02230	0.02520	0.01280	0.02890	0.03190
26.20000	4.21080	0.02430	0.34910	0.03730	0.02280	0.02550	0.01290	0.02880	0.03210
26.40000	4.21130	0.02360	0.34920	0.03450	0.02330	0.02570	0.01300	0.02880	0.03240
26.60000	4.21170	0.02290	0.34930	0.03160	0.02390	0.02590	0.01300	0.02880	0.03260

26.80000	4.21220	0.02220	0.34930	0.02880	0.02430	0.02610	0.01280	0.02900	0.03280
27.00000	4.21260	0.02160	0.34940	0.02600	0.02470	0.02620	0.01250	0.02920	0.03300
27.20000	4.21300	0.02090	0.34940	0.02330	0.02490	0.02620	0.01200	0.02950	0.03310
27.40000	4.21340	0.02030	0.34940	0.02070	0.02500	0.02630	0.01140	0.02990	0.03320
27.60000	4.21380	0.01970	0.34940	0.01820	0.02480	0.02630	0.01070	0.03030	0.03340
27.80000	4.21420	0.01910	0.34940	0.01600	0.02450	0.02620	0.00970	0.03080	0.03350
28.00000	4.21460	0.01850	0.34940	0.01400	0.02400	0.02620	0.00870	0.03130	0.03350
28.20000	4.21490	0.01790	0.34940	0.01230	0.02340	0.02610	0.00750	0.03180	0.03340
28.40000	4.21530	0.01730	0.34940	0.01070	0.02270	0.02590	0.00630	0.03230	0.03330
28.60000	4.21560	0.01680	0.34940	0.00940	0.02190	0.02580	0.00500	0.03270	0.03300
28.80000	4.21600	0.01620	0.34940	0.00820	0.02100	0.02560	0.00380	0.03310	0.03220
29.00000	4.21630	0.01570	0.34940	0.00720	0.02010	0.02540	0.00270	0.03340	0.03060
29.20000	4.21660	0.01520	0.34940	0.00640	0.01930	0.02520	0.00160	0.03370	0.02720
29.40000	4.21690	0.01470	0.34930	0.00560	0.01840	0.02500	0.00060	0.03400	0.02080
29.60000	4.21720	0.01420	0.34930	0.00500	0.01750	0.02480	0.00030	0.03430	0.01270
29.80000	4.21750	0.01370	0.34930	0.00440	0.01660	0.02450	0.00110	0.03450	0.00640
30.00000	4.21780	0.01330	0.34920	0.00390	0.01580	0.02430	-0.00180	0.03470	0.00260
30.20000	4.21800	0.01280	0.34920	0.00350	0.01500	0.02400	-0.00240	0.03490	0.00030
30.40000	4.21830	0.01240	0.34920	0.00310	0.01420	0.02380	-0.00290	0.03510	0.00120
30.60000	4.21860	0.01200	0.34910	0.00280	0.01340	0.02350	-0.00340	0.03530	0.00210
30.80000	4.21880	0.01160	0.34910	0.00250	0.01270	0.02320	-0.00380	0.03550	0.00280
31.00000	4.21910	0.01120	0.34910	0.00220	0.01200	0.02290	-0.00420	0.03570	0.00330
31.20000	4.21930	0.01080	0.34900	0.00200	0.01130	0.02260	-0.00460	0.03580	0.00360
31.40000	4.21950	0.01040	0.34900	0.00180	0.01070	0.02240	-0.00490	0.03600	0.00380
31.60000	4.21980	0.01010	0.34890	0.00160	0.01000	0.02210	-0.00520	0.03620	0.00400
31.80000	4.22000	0.00970	0.34890	0.00140	0.00940	0.02180	-0.00540	0.03640	0.00410
32.00000	4.22020	0.00940	0.34890	0.00130	0.00890	0.02150	-0.00560	0.03660	0.00420
32.20000	4.22040	0.00910	0.34880	0.00110	0.00830	0.02120	-0.00590	0.03670	0.00420
32.40000	4.22060	0.00870	0.34880	0.00100	0.00780	0.02090	-0.00600	0.03690	0.00430
32.60000	4.22080	0.00840	0.34880	0.00090	0.00730	0.02060	-0.00620	0.03710	0.00430
32.80000	4.22100	0.00810	0.34870	0.00080	0.00680	0.02030	-0.00640	0.03720	0.00430
33.00000	4.22120	0.00790	0.34870	0.00070	0.00640	0.02010	-0.00650	0.03740	0.00430
33.20000	4.22140	0.00760	0.34860	0.00060	0.00600	0.01980	-0.00660	0.03760	0.00430
33.40000	4.22160	0.00730	0.34860	0.00060	0.00550	0.01950	-0.00680	0.03770	0.00420
33.60000	4.22180	0.00710	0.34860	0.00050	0.00520	0.01920	-0.00690	0.03780	0.00420
33.80000	4.22190	0.00680	0.34850	0.00040	0.00480	0.01900	-0.00700	0.03800	0.00420
34.00000	4.22210	0.00660	0.34850	0.00040	0.00450	0.01870	-0.00710	0.03810	0.00410
34.20000	4.22230	0.00640	0.34850	0.00030	0.00410	0.01840	-0.00720	0.03820	0.00410
34.40000	4.22240	0.00620	0.34840	0.00030	0.00380	0.01810	-0.00720	0.03830	0.00400
34.60000	4.22260	0.00600	0.34840	0.00030	0.00350	0.01790	-0.00730	0.03840	0.00400
34.80000	4.22270	0.00580	0.34840	0.00020	0.00330	0.01760	-0.00740	0.03850	0.00390
35.00000	4.22290	0.00560	0.34830	0.00020	0.00300	0.01740	-0.00740	0.03860	0.00390
35.20000	4.22300	0.00540	0.34830	0.00020	0.00280	0.01710	-0.00740	0.03870	0.00380
35.40000	4.22320	0.00520	0.34830	0.00010	0.00260	0.01690	-0.00750	0.03870	0.00380
35.60000	4.22330	0.00500	0.34820	0.00010	0.00240	0.01660	-0.00750	0.03880	0.00370
35.80000	4.22350	0.00490	0.34820	0.00010	0.00220	0.01640	-0.00750	0.03880	0.00370
36.00000	4.22360	0.00470	0.34820	0.00010	0.00200	0.01610	-0.00760	0.03880	0.00360
36.20000	4.22370	0.00460	0.34810	0.00010	0.00180	0.01590	-0.00760	0.03890	0.00350
36.40000	4.22390	0.00440	0.34810	0.00000	0.00170	0.01570	-0.00750	0.03880	0.00350
36.60000	4.22400	0.00430	0.34810	0.00000	0.00150	0.01540	-0.00750	0.03880	0.00340

36.80000	4.22410	0.00420	0.34810	0.00000	0.00140	0.01520	-0.00750	0.03880	0.00340
37.00000	4.22420	0.00400	0.34800	0.00000	0.00120	0.01500	-0.00750	0.03880	0.00330
37.20000	4.22430	0.00390	0.34800	0.00000	0.00110	0.01480	-0.00750	0.03870	0.00330
37.40000	4.22450	0.00380	0.34800	0.00000	0.00100	0.01450	-0.00750	0.03870	0.00320
37.60000	4.22460	0.00370	0.34800	0.00000	0.00090	0.01430	-0.00740	0.03860	0.00320
37.80000	4.22470	0.00360	0.34800	0.00000	0.00080	0.01410	-0.00740	0.03850	0.00310
38.00000	4.22480	0.00350	0.34790	0.00000	0.00070	0.01390	-0.00740	0.03840	0.00310
38.20000	4.22490	0.00340	0.34790	0.00000	0.00070	0.01360	-0.00730	0.03830	0.00300
38.40000	4.22500	0.00330	0.34790	0.00000	0.00060	0.01340	-0.00730	0.03820	0.00300
38.60000	4.22510	0.00320	0.34790	0.00000	0.00050	0.01320	-0.00720	0.03810	0.00290
38.80000	4.22520	0.00310	0.34790	0.00000	0.00040	0.01300	-0.00720	0.03790	0.00290
39.00000	4.22530	0.00300	0.34780	-0.00010	0.00040	0.01280	-0.00710	0.03770	0.00280
39.20000	4.22540	0.00290	0.34780	-0.00010	0.00030	0.01260	-0.00700	0.03760	0.00280
39.40000	4.22550	0.00280	0.34780	-0.00010	0.00030	0.01240	-0.00700	0.03740	0.00270
39.60000	4.22560	0.00270	0.34780	-0.00010	0.00020	0.01220	-0.00690	0.03720	0.00270
39.80000	4.22570	0.00270	0.34780	-0.00010	0.00020	0.01200	-0.00680	0.03700	0.00270
40.00000	4.22580	0.00260	0.34780	-0.00010	0.00020	0.01180	-0.00670	0.03670	0.00260

Transition electric dipole moment (in a.u.) starting from the Rb_2 ground state (singlet Sigma_g^+) towards the 6 lowest singlet Sigma_u^+ states (labelled as (1) to (6)), as functions of the internuclear distance R (in a.u.).

#R	(1)	(2)	(3)	(4)	(5)	(6)
52.000	39.525	-0.3894	-0.1222	-0.1378	-0.0209	0.0873
54.000	39.923	-0.3686	-0.2031	-0.1304	-0.0604	0.0877
56.000	40.286	-0.3448	-0.2716	-0.1249	-0.0972	0.0929
60.000	40.963	-0.2987	-0.3733	-0.1185	-0.1617	0.1153
62.000	41.304	-0.2778	-0.4089	-0.1171	-0.1879	0.1296
64.000	41.659	-0.2581	-0.4361	-0.1163	-0.2094	0.1446
66.000	42.037	-0.2387	-0.4566	-0.1159	-0.2259	0.159
68.000	42.440	-0.2192	-0.4719	-0.1155	-0.2377	0.1725
70.000	42.872	-0.1989	-0.4831	-0.1149	-0.2455	0.1849
72.000	43.331	-0.1775	-0.4915	-0.1138	-0.2498	0.1965
74.000	43.815	-0.1546	-0.4977	-0.1123	-0.2515	0.2074
76.000	44.320	-0.1301	-0.5023	-0.1103	-0.2511	0.2181
78.000	44.842	-0.1038	-0.5057	-0.1079	-0.2493	0.2284
80.000	45.374	-0.0756	-0.5082	-0.1051	-0.2464	0.2379
82.000	45.911	-0.0456	-0.5099	-0.1019	-0.243	0.2458
84.000	46.445	-0.0137	-0.5108	-0.0987	-0.2393	0.251
86.000	46.970	0.02	-0.511	-0.0954	-0.2355	0.2522
88.000	47.478	0.0556	-0.5105	-0.0923	-0.2318	0.2487
90.000	47.963	0.093	-0.5092	-0.0896	-0.2284	0.2401
94.000	48.833	0.1726	-0.5041	-0.0857	-0.2225	0.2068
96.000	49.205	0.2147	-0.5001	-0.0848	-0.2196	0.1818
98.000	49.526	0.258	-0.4952	-0.0841	-0.2158	0.1512
100.000	49.793	0.3024	-0.4892	-0.0831	-0.2098	0.1161
102.000	50.000	0.3478	-0.4821	-0.0803	-0.1999	0.0787
104.000	50.145	0.3939	-0.4739	-0.0736	-0.1851	0.0434
106.000	50.227	0.4405	-0.4644	-0.0612	-0.1671	0.0141
108.000	50.245	0.4875	-0.4536	-0.0424	-0.1486	-0.0074
110.000	50.201	0.5345	-0.4413	-0.0178	-0.1318	-0.0217
112.000	50.098	0.5813	-0.4275	0.0113	-0.1178	-0.0305
114.000	49.939	0.6277	-0.412	0.0433	-0.1062	-0.0351
116.000	49.731	0.6733	-0.3946	0.0771	-0.0966	-0.0366
118.000	49.480	0.7179	-0.3753	0.1113	-0.0884	-0.0358
120.000	49.191	0.761	-0.3539	0.1451	-0.0813	-0.0334
122.000	48.873	0.8024	-0.3308	0.1775	-0.0748	-0.0295
124.000	48.532	0.8417	-0.306	0.2076	-0.0687	-0.0244
126.000	48.176	0.8785	-0.2803	0.2348	-0.063	-0.0183
128.000	47.812	0.9125	-0.2542	0.2586	-0.0574	-0.0113
130.000	47.446	0.9434	-0.2285	0.2789	-0.052	-0.0036
132.000	47.083	0.9709	-0.2037	0.2957	-0.0468	-0.0048
134.000	46.729	0.9948	-0.1803	0.3091	-0.0417	-0.0137
136.000	46.387	10.149	-0.1588	0.3196	-0.0369	-0.023
138.000	46.063	10.310	-0.1391	0.3275	-0.0325	-0.0325
140.000	45.757	10.431	-0.1214	0.3331	-0.0285	-0.042
142.000	45.472	10.511	-0.1056	0.3369	-0.0257	-0.0515
144.000	45.209	10.550	-0.0916	0.339	0.028	-0.0592

146.000	44.970	10.548	-0.0791	0.3396	0.0741	-0.0031
148.000	44.753	10.507	-0.0681	0.3391	0.0831	-0.005
150.000	44.559	10.429	-0.0583	0.3376	0.0925	-0.0038
152.000	44.386	10.315	-0.0496	0.3351	0.1018	-0.0016
154.000	44.234	10.168	-0.042	0.332	0.111	0.0008
156.000	44.102	0.999	-0.0352	0.3281	0.12	0.0032
158.000	43.986	0.9785	-0.0291	0.3238	0.1286	0.0056
160.000	43.886	0.9556	-0.0237	0.319	0.1369	0.008
162.000	43.800	0.9306	-0.0189	0.3138	0.1449	0.0104
164.000	43.726	0.9039	-0.0145	0.3084	0.1525	0.0129
166.000	43.663	0.8758	-0.0106	0.3027	0.1598	0.0154
168.000	43.609	0.8466	-0.007	0.2968	0.1667	0.0182
170.000	43.562	0.8167	-0.0038	0.2908	0.1733	0.0211
172.000	43.521	0.7863	-0.0009	0.2848	0.1796	0.0242
174.000	43.485	0.7557	0.0018	0.2787	0.1857	0.0277
176.000	43.453	0.7252	0.0043	0.2726	0.1914	0.0314
178.000	43.424	0.695	0.0066	0.2666	0.1969	0.0355
180.000	43.397	0.6652	0.0088	0.2606	0.2022	0.0398
182.000	43.372	0.636	0.0109	0.2547	0.2073	0.0438
184.000	43.349	0.6075	0.0128	0.2489	0.2122	0.047
186.000	43.327	0.5799	0.0147	0.2433	0.2169	0.049
188.000	43.305	0.5532	0.0166	0.2378	0.2215	0.0503
190.000	43.285	0.5274	0.0184	0.2324	0.2259	0.0514
192.000	43.264	0.5026	0.0202	0.2273	0.2302	0.0525
194.000	43.244	0.4788	0.022	0.2223	0.2343	0.0535
196.000	43.225	0.456	0.0238	0.2175	0.2383	0.0545
198.000	43.205	0.4341	0.0257	0.2129	0.2422	0.0558
200.000	43.186	0.4133	0.0276	0.2085	0.246	0.057
202.000	43.167	0.3933	0.0296	0.2044	0.2496	0.0583
204.000	43.148	0.3742	0.0316	0.2004	0.2532	0.0595
206.000	43.130	0.356	0.0338	0.1967	0.2567	0.0607
208.000	43.112	0.3385	0.036	0.1932	0.2601	0.0618
210.000	43.094	0.3218	0.0383	0.1899	0.2634	0.0628
212.000	43.076	0.3057	0.0407	0.1868	0.2666	0.0638
214.000	43.059	0.2903	0.0433	0.184	0.2697	0.0646
216.000	43.042	0.2754	0.0459	0.1813	0.2727	0.0654
218.000	43.025	0.2611	0.0485	0.1789	0.2757	0.0658
220.000	43.009	0.2472	0.0512	0.1767	0.2785	0.0664
224.000	42.977	0.2206	0.0565	0.1729	0.284	0.0673
226.000	42.962	0.2078	0.059	0.1712	0.2864	0.0673
228.000	42.947	0.1954	0.0612	0.1697	0.2889	0.0675
230.000	42.932	0.1834	0.0631	0.1683	0.2914	0.0676
234.000	42.904	0.1604	0.0654	0.1658	0.296	0.0676
236.000	42.891	0.1497	0.0657	0.1647	0.2982	0.0675
238.000	42.877	0.1394	0.0654	0.1635	0.3003	0.0673
240.000	42.864	0.1298	0.0644	0.1623	0.3023	0.067
242.000	42.852	0.1208	0.0628	0.1612	0.3042	0.0666
244.000	42.840	0.1124	0.0607	0.1599	0.306	0.0661
246.000	42.828	0.1047	0.0581	0.1585	0.3078	0.0656
248.000	42.816	0.0976	0.0552	0.1571	0.3095	0.065

250.000	42.805	0.0912	0.0521	0.1555	0.3111	0.0643
252.000	42.794	0.0853	0.0489	0.1539	0.3126	0.0635
254.000	42.783	0.0799	0.0456	0.1521	0.314	0.0627
256.000	42.772	0.075	0.0423	0.1502	0.3154	0.0618
258.000	42.762	0.0706	0.0391	0.1483	0.3167	0.0608
260.000	42.752	0.0666	0.036	0.1463	0.3179	0.0598
262.000	42.743	0.0628	0.0331	0.1443	0.3191	0.0587
264.000	42.733	0.0595	0.0304	0.1423	0.3202	0.0576
266.000	42.724	0.0563	0.0278	0.1402	0.3212	0.0564
268.000	42.715	0.0535	0.0255	0.1382	0.3222	0.0551
270.000	42.707	0.0508	0.0233	0.1362	0.3231	0.0538
272.000	42.698	0.0484	0.0213	0.1343	0.324	0.0525
274.000	42.690	0.0461	0.0195	0.1324	0.3248	0.0511
276.000	42.682	0.0439	0.0178	0.1305	0.3255	0.0497
278.000	42.674	0.042	0.0163	0.1288	0.3262	0.0482
280.000	42.667	0.0401	0.0149	0.1271	0.3268	0.0468
282.000	42.659	0.0384	0.0137	0.1255	0.3274	0.0452
284.000	42.652	0.0367	0.0125	0.1239	0.3279	0.0437
286.000	42.645	0.0352	0.0115	0.1225	0.3284	0.0422
288.000	42.638	0.0337	0.0106	0.1211	0.3288	0.0406
290.000	42.632	0.0323	0.0097	0.1199	0.3292	0.039
292.000	42.625	0.031	0.009	0.1187	0.3296	0.0374
294.000	42.619	0.0298	0.0083	0.1177	0.3299	0.0358
296.000	42.613	0.0286	0.0077	0.1167	0.3302	0.0342
298.000	42.607	0.0275	0.0071	0.1158	0.3304	0.0326
300.000	42.601	0.0264	0.0066	0.115	0.3306	0.031
302.000	42.595	0.0254	0.0061	0.1144	0.3307	0.0294
304.000	42.590	0.0244	0.0057	0.1138	0.3309	0.0278
306.000	42.584	0.0235	0.0053	0.1134	0.3309	0.0263
308.000	42.579	0.0226	0.005	0.113	0.331	0.0247
310.000	42.574	0.0218	0.0047	0.1128	0.331	0.0231
312.000	42.569	0.021	0.0044	0.1127	0.3309	0.0216
314.000	42.564	0.0202	0.0041	0.1127	0.3308	0.0201
316.000	42.560	0.0195	0.0039	0.1129	0.3307	0.0186
318.000	42.555	0.0188	0.0037	0.1132	0.3305	0.0172
320.000	42.550	0.0181	0.0035	0.1136	0.3303	0.0157
322.000	42.546	0.0175	0.0033	0.1142	0.33	0.0143
324.000	42.542	0.0169	0.0031	0.1149	0.3296	0.013
326.000	42.538	0.0163	0.003	0.1158	0.3292	0.0116
328.000	42.534	0.0158	0.0028	0.1169	0.3288	0.0103
330.000	42.530	0.0152	0.0027	0.1182	0.3282	0.009
332.000	42.526	0.0147	0.0026	0.1197	0.3276	0.0078
334.000	42.522	0.0142	0.0025	0.1214	0.3269	0.0066
336.000	42.518	0.0138	0.0024	0.1234	0.3261	0.0054
338.000	42.515	0.0133	0.0023	0.1257	0.3251	0.0043
340.000	42.511	0.0129	0.0023	0.1283	0.3241	0.0032
342.000	42.508	0.0125	0.0022	0.1312	0.3228	0.0022
344.000	42.505	0.0121	0.0021	0.1344	0.3214	0.0011
346.000	42.501	0.0117	0.0021	0.1381	0.3198	-0.0002
348.000	42.498	0.0113	0.002	0.1423	0.3179	-0.0008

350.000	42.495	0.011	0.0019	0.1469	0.3157	-0.0017
352.000	42.492	0.0107	0.0019	0.1522	0.3131	-0.0025
354.000	42.489	0.0104	0.0018	0.158	0.3102	-0.0034
356.000	42.486	0.0101	0.0018	0.1646	0.3067	-0.0042
358.000	42.483	0.0098	0.0018	0.1719	0.3026	-0.0049
360.000	42.481	0.0095	0.0017	0.18	0.2978	-0.0056
362.000	42.478	0.0092	0.0017	0.189	0.2921	-0.0063
364.000	42.475	0.009	0.0017	0.1988	0.2855	-0.007
366.000	42.473	0.0087	0.0016	0.2095	0.2777	-0.0076
368.000	42.470	0.0085	0.0016	0.2209	0.2686	-0.0081
370.000	42.468	0.0083	0.0016	0.2329	0.2583	-0.0087
372.000	42.465	0.008	0.0015	0.2452	0.2466	-0.0092
374.000	42.463	0.0078	0.0015	0.2575	0.2337	-0.0097
376.000	42.461	0.0076	0.0015	0.2694	0.2198	-0.0102
378.000	42.459	0.0074	0.0015	0.2806	0.2053	-0.0106
380.000	42.456	0.0072	0.0014	0.2908	0.1906	-0.011
382.000	42.454	0.0071	0.0014	0.2998	0.176	-0.0114
394.000	42.442	0.0061	0.0013	0.3312	0.1053	-0.0131
396.000	42.440	0.006	0.0013	0.3337	0.0969	-0.0133
398.000	42.439	0.0058	0.0013	0.3358	0.0893	-0.0135
400.000	42.437	0.0057	0.0012	0.3375	0.0825	-0.0137

Transition electric dipole moment (in a.u.) starting from the Rb_2 lowest triplet Sigma_u^+ state towards the 5 lowest triplet Sigma_g^+ states (labelled as (1) to (5)), as functions of the internuclear distance R (in a.u.).

#R	(1)	(2)	(3)	(4)	(5)
5.2	3.92460	-0.93280	-0.24210	-0.61350	0.08000
5.4	3.96530	-1.00560	-0.14230	-0.67000	0.02700
5.6	4.03260	-1.02750	0.02010	-0.71310	0.06540
6	4.25150	-0.79980	0.65750	-0.34260	0.45230
6.2	4.38210	-0.50420	0.72340	-0.11140	0.56700
6.4	4.49140	0.11750	0.70840	0.01370	0.55640
6.8	4.59980	0.60190	0.63130	0.09310	0.45550
7	4.62650	0.83510	0.58580	0.12760	0.40390
7.2	4.65250	0.98650	0.54050	0.15440	0.35700
7.4	4.68110	1.07620	0.49750	0.17530	0.31530
7.6	4.71170	1.12200	0.45780	0.19150	0.27840
7.8	4.74260	1.13740	0.42190	0.20380	0.24570
8	4.77230	1.13150	0.38970	0.21310	0.21670
8.2	4.79960	1.11120	0.36120	0.21980	0.19060
8.4	4.82360	1.08100	0.33610	0.22460	0.16690
8.6	4.84410	1.04430	0.31400	0.22780	0.14500
8.8	4.86060	1.00360	0.29440	0.22990	0.12440
9	4.87330	0.96060	0.27700	0.23120	0.10480
9.4	4.88750	0.87260	0.24710	0.23250	0.06720
9.6	4.88940	0.82930	0.23390	0.23320	0.04900
9.8	4.88820	0.78710	0.22140	0.23410	0.03130
10	4.88400	0.74640	0.20930	0.23570	0.17380
10.2	4.87730	0.70740	0.19740	0.23810	0.00110
10.4	4.86830	0.67030	0.18540	0.24170	-0.01480
10.6	4.85720	0.63500	0.17320	0.24660	-0.02600
10.8	4.84440	0.60180	0.16060	0.25300	-0.03390
11.2	4.81460	0.54110	0.13390	0.27010	-0.03830
11.4	4.79810	0.51360	0.11970	0.28010	-0.03510
11.6	4.78070	0.48790	0.10500	0.29020	-0.02950
11.8	4.76280	0.46410	0.09000	0.30000	-0.02280
12	4.74440	0.44190	0.07480	0.30900	-0.01630
12.2	4.72590	0.42150	0.05980	0.31720	-0.01080
12.4	4.70720	0.40260	0.04510	0.32450	-0.00670
12.6	4.68860	0.38530	0.03100	0.33100	-0.00400
12.8	4.67020	0.36950	0.01780	0.33680	-0.00260
13	4.65210	0.35510	0.00570	0.34190	-0.00230
13.2	4.63430	0.34200	0.00520	0.34660	-0.00270
13.4	4.61690	0.33010	0.01470	0.35080	-0.00340
13.6	4.60010	0.31940	0.02270	0.35460	-0.00410
13.8	4.58380	0.30970	0.02930	0.35820	-0.00430
14	4.56810	0.30100	0.03450	0.36160	-0.00390
14.2	4.55300	0.29320	0.03830	0.36480	-0.00270
14.4	4.53850	0.28600	0.04090	0.36780	0.00080

14.6	4.52470	0.27950	0.04240	0.37060	0.00170
14.8	4.51150	0.27350	0.04300	0.37320	0.00470
15	4.49890	0.26790	0.04290	0.37550	0.00790
15.2	4.48690	0.26250	0.04210	0.37770	0.01120
15.4	4.47560	0.25730	0.04100	0.37960	0.01440
15.6	4.46480	0.25220	0.03970	0.38130	0.01730
15.8	4.45460	0.24710	0.03820	0.38270	0.01990
16	4.44490	0.24210	0.03680	0.38390	0.02200
16.2	4.43580	0.23700	0.03540	0.38490	0.02370
16.4	4.42710	0.23190	0.03410	0.38570	0.02490
16.6	4.41890	0.22680	0.03290	0.38630	0.02580
16.8	4.41120	0.22160	0.03190	0.38670	0.02630
17	4.40390	0.21630	0.03100	0.38690	0.02650
17.2	4.39700	0.21110	0.03020	0.38690	0.02650
17.4	4.39040	0.20580	0.02960	0.38670	0.02630
17.6	4.38420	0.20050	0.02900	0.38640	0.02600
17.8	4.37840	0.19520	0.02850	0.38600	0.02550
18	4.37280	0.18990	0.02810	0.38540	0.02510
18.2	4.36760	0.18470	0.02770	0.38460	0.02450
18.4	4.36260	0.17950	0.02740	0.38380	0.02400
18.6	4.35790	0.17430	0.02700	0.38290	0.02350
18.8	4.35340	0.16920	0.02670	0.38190	0.02300
19	4.34910	0.16420	0.02640	0.38080	0.02260
19.2	4.34510	0.15930	0.02610	0.37960	0.02220
19.4	4.34120	0.15440	0.02570	0.37850	0.02190
19.6	4.33760	0.14960	0.02540	0.37720	0.02160
19.8	4.33410	0.14490	0.02500	0.37600	0.02150
20	4.33080	0.14040	0.02460	0.37470	0.02140
20.2	4.32760	0.13590	0.02420	0.37340	0.02140
20.4	4.32460	0.13150	0.02380	0.37220	0.02150
20.6	4.32170	0.12720	0.02340	0.37090	0.02160
20.8	4.31900	0.12300	0.02290	0.36960	0.02190
21	4.31630	0.11900	0.02240	0.36840	0.02220
21.2	4.31380	0.11500	0.02190	0.36710	0.02250
21.4	4.31140	0.11120	0.02140	0.36590	0.02300
21.6	4.30910	0.10740	0.02090	0.36470	0.02340
21.8	4.30690	0.10380	0.02030	0.36360	0.02390
22	4.30480	0.10030	0.01980	0.36250	0.02440
22.4	4.30080	0.09360	0.01860	0.36030	0.02550
22.6	4.29890	0.09040	0.01800	0.35930	0.02600
22.8	4.29710	0.08730	0.01750	0.35830	0.02650
23	4.29540	0.08430	0.01690	0.35740	0.02700
23.4	4.29210	0.07870	0.01570	0.35560	0.02800
23.6	4.29060	0.07600	0.01510	0.35480	0.02840
23.8	4.28910	0.07340	0.01460	0.35410	0.02880
24	4.28760	0.07090	0.01400	0.35330	0.02920
24.2	4.28620	0.06850	0.01350	0.35260	0.02950
24.4	4.28490	0.06620	0.01290	0.35200	0.02980
24.6	4.28360	0.06390	0.01240	0.35130	0.03010
24.8	4.28230	0.06180	0.01190	0.35070	0.03030

25	4.28110	0.05970	0.01140	0.35020	0.03050
25.2	4.27990	0.05770	0.01090	0.34970	0.03070
25.4	4.27880	0.05570	0.01040	0.34920	0.03080
25.6	4.27770	0.05380	0.01000	0.34870	0.03090
25.8	4.27660	0.05200	0.00950	0.34830	0.03090
26	4.27560	0.05030	0.00910	0.34790	0.03100
26.2	4.27460	0.04860	0.00870	0.34760	0.03100
26.4	4.27360	0.04690	0.00830	0.34720	0.03090
26.6	4.27270	0.04540	0.00790	0.34690	0.03090
26.8	4.27170	0.04380	0.00760	0.34660	0.03080
27	4.27080	0.04240	0.00720	0.34640	0.03070
27.2	4.27000	0.04090	0.00690	0.34610	0.03060
27.4	4.26910	0.03950	0.00660	0.34590	0.03040
27.6	4.26830	0.03820	0.00630	0.34570	0.03030
27.8	4.26750	0.03690	0.00600	0.34550	0.03010
28	4.26680	0.03570	0.00570	0.34540	0.03000
28.2	4.26600	0.03440	0.00540	0.34520	0.02980
28.4	4.26530	0.03330	0.00520	0.34510	0.02960
28.6	4.26460	0.03210	0.00500	0.34500	0.02940
28.8	4.26390	0.03100	0.00470	0.34490	0.02920
29	4.26320	0.03000	0.00450	0.34480	0.02900
29.2	4.26260	0.02890	0.00430	0.34470	0.02890
29.4	4.26190	0.02790	0.00410	0.34470	0.02870
29.6	4.26130	0.02700	0.00400	0.34460	0.02850
29.8	4.26070	0.02600	0.00380	0.34460	0.02830
30	4.26010	0.02510	0.00360	0.34450	0.02810
30.2	4.25960	0.02430	0.00350	0.34450	0.02800
30.4	4.25900	0.02340	0.00340	0.34450	0.02780
30.6	4.25850	0.02260	0.00320	0.34450	0.02760
30.8	4.25790	0.02190	0.00310	0.34450	0.02750
31	4.25740	0.02110	0.00300	0.34450	0.02730
31.2	4.25690	0.02040	0.00290	0.34450	0.02720
31.4	4.25640	0.01970	0.00280	0.34450	0.02700
31.6	4.25600	0.01900	0.00270	0.34450	0.02690
31.8	4.25550	0.01840	0.00260	0.34460	0.02680
32.2	4.25460	0.01720	0.00240	0.34460	0.02660
32.4	4.25420	0.01660	0.00240	0.34470	0.02640
32.6	4.25380	0.01600	0.00230	0.34470	0.02630
32.8	4.25340	0.01550	0.00220	0.34470	0.02620
33	4.25300	0.01500	0.00220	0.34480	0.02610
34.2	4.25080	0.01240	0.00190	0.34510	0.02550
34.4	4.25050	0.01200	0.00190	0.34510	0.02540
34.6	4.25010	0.01160	0.00180	0.34520	0.02530
34.8	4.24980	0.01130	0.00180	0.34520	0.02520
35	4.24950	0.01090	0.00180	0.34530	0.02510
35.6	4.24860	0.01000	0.00170	0.34550	0.02470
35.8	4.24830	0.00970	0.00170	0.34550	0.02460
36	4.24810	0.00950	0.00160	0.34560	0.02450
36.2	4.24780	0.00920	0.00160	0.34560	0.02430
36.4	4.24750	0.00890	0.00160	0.34570	0.02420

36.6	4.24730	0.00870	0.00160	0.34580	0.02410
36.8	4.24700	0.00850	0.00150	0.34580	0.02390
37	4.24680	0.00820	0.00150	0.34590	0.02380
37.2	4.24650	0.00800	0.00150	0.34590	0.02360
37.4	4.24630	0.00780	0.00150	0.34600	0.02350
37.6	4.24610	0.00760	0.00150	0.34600	0.02330
37.8	4.24590	0.00740	0.00140	0.34610	0.02310
38	4.24560	0.00720	0.00140	0.34610	0.02300
38.2	4.24540	0.00710	0.00140	0.34620	0.02280
39.4	4.24420	0.00610	0.00130	0.34640	0.02170
39.6	4.24400	0.00600	0.00130	0.34650	0.02150
39.8	4.24390	0.00580	0.00120	0.34650	0.02130
40	4.24370	0.00570	0.00120	0.34650	0.02110

Table: Parameters for the fit of the dynamic polarizability of the vibrational levels v (with N=0) of the lowest triplet Sigma_u^+ state of Rb_2, using the ansatz of the paper with two effective transitions. omega_eff: effective frequency; d_eff: effective dipole moment. The frequency ranges taken in account for the fit are indicated as intervals.

#	1st effective transition v (cm^-1)	omega_eff/(2*pi*c) d_eff (a.u.)	2nd effective transition omega_eff/(2*pi*c) d_eff (a.u.)	rRMS (%)	frequency domains included in the fit (cm^-1)
0	10112.33	2.792881	13481.32	3.211023	0.976 [0.00 ; 9527.06] [11017.65 ; 13172.54] [13698.11 ; 14500.00]
1	10124.48	2.806632	13462.41	3.186648	2.402 [0.00 ; 9514.01] [11172.08 ; 13131.21] [13719.14 ; 14500.00]
2	10138.02	2.819581	13442.32	3.161026	4.702 [0.00 ; 9501.68] [11239.51 ; 13118.89] [13724.94 ; 14500.00]
3	10149.23	2.826924	13422.63	3.136275	7.265 [0.00 ; 9489.36] [11332.32 ; 13106.56] [13738.71 ; 14500.00]
4	10165.60	2.836308	13403.04	3.113487	9.453 [0.00 ; 9477.03] [11396.12 ; 13094.24] [13792.36 ; 14500.00]
5	10178.56	2.839702	13384.04	3.092283	11.806 [0.00 ; 9465.43] [11483.12 ; 13082.64] [13765.54 ; 14500.00]
6	10193.00	2.841532	13365.39	3.073084	13.520 [0.00 ; 9453.83] [11567.95 ; 13071.04] [13761.19 ; 14500.00]
7	10209.01	2.842671	13346.88	3.055347	13.608 [0.00 ; 9442.95] [11648.43 ; 13060.16] [13766.26 ; 14500.00]
8	10241.94	2.856396	13327.47	3.038251	15.856 [0.00 ; 9432.80] [11683.23 ; 13050.01] [13803.97 ; 14500.00]
9	10255.95	2.850516	13309.78	3.024335	12.723 [0.00 ; 9422.65] [11780.39 ; 13039.86] [13794.54 ; 14500.00]
10	10297.71	2.865961	13290.31	3.009602	13.416 [0.00 ; 9413.23] [11812.29 ; 13030.43] [13775.69 ; 14500.00]
11	10337.01	2.875559	13271.41	2.997182	14.456 [0.00 ; 9403.80] [11863.77 ; 13021.01] [13766.99 ; 14500.00]
12	10649.49	2.912128	13315.06	3.254995	14.369 [0.00 ; 9394.38] [11933.37 ; 13011.58] [13774.96 ; 14340.57]
13	10743.27	2.917850	13297.31	3.267539	10.163 [0.00 ; 9385.68] [11999.35 ; 13002.88] [13774.96 ; 14331.87]
14	10856.18	2.925106	13279.06	3.281925	9.215 [0.00 ; 9377.70] [12044.30 ; 12986.93] [13774.96 ; 14273.87]
15	10952.70	2.930383	13257.34	3.281501	8.486 [0.00 ; 9369.73] [12088.53 ; 12965.91] [13812.67 ; 14315.92]
16	11067.05	2.919322	13243.23	3.309404	7.851 [0.00 ; 9362.48] [12146.53 ; 12941.25] [13769.16 ; 14258.65]
17	11171.55	2.918061	13220.90	3.312712	7.547 [0.00 ; 9355.23] [12186.41 ; 12921.68] [13798.89 ; 14252.12]
18	11272.00	2.907345	13201.39	3.324143	7.232 [0.00 ; 9348.70] [12239.34 ; 12899.20] [13801.07 ; 14245.59]
19	11385.70	2.889403	13182.66	3.345595	7.046 [0.00 ; 9342.90] [12289.36 ; 12884.70] [13776.41 ; 14239.07]
20	11474.75	2.868762	13164.56	3.358371	6.764 [0.00 ; 9336.37] [12349.54 ; 12852.80] [13770.61 ; 14233.27]
21	11589.59	2.857391	13139.36	3.366384	6.569 [0.00 ; 9331.30] [12368.39 ; 12847.72] [13793.09 ; 14177.44]
22	11676.27	2.840077	13117.14	3.371518	6.251 [0.00 ; 9326.22] [12422.05 ; 12828.87] [13807.59 ; 14172.37]
23	11768.03	2.814790	13096.43	3.383873	5.906 [0.00 ; 9321.15] [12460.47 ; 12804.95] [13793.09 ; 14218.04]
24	11863.93	2.790719	13073.29	3.395242	5.583 [0.00 ; 9317.52] [12485.85 ; 12794.07] [13789.46 ; 14213.69]
25	11948.75	2.764104	13051.38	3.406065	5.242 [0.00 ; 9313.17] [12519.93 ; 12770.15] [13804.69 ; 14109.29]
26	12023.87	2.743002	13027.71	3.407386	4.795 [0.00 ; 9309.55] [12551.83 ; 12750.57] [13811.94 ; 14156.42]
27	12106.93	2.707386	13005.36	3.423806	4.397 [0.00 ; 9306.65] [12588.08 ; 12744.77] [13788.74 ; 14152.79]
28	11037.87	2.367592	13099.24	3.476488	1.415 [0.00 ; 9303.75] [12647.53 ; 12722.29] [13815.57 ; 14099.86]
29	11080.24	2.345712	13089.80	3.479831	1.210 [0.00 ; 9301.57] [12651.88 ; 12703.44] [13773.51 ; 14147.71]
30	11079.21	2.253547	13062.51	3.533553	1.059 [0.00 ; 9299.40] [12684.51 ; 12695.47] [13780.76 ; 14145.54]
31	9911.65	0.936293	12846.40	4.140226	0.408 [0.00 ; 9297.95] [13769.16 ; 14144.09]
32	9907.44	0.841004	12826.29	4.160146	0.335 [0.00 ; 9296.50] [13768.44 ; 14142.64]
33	9862.64	0.714259	12804.07	4.184604	0.241 [0.00 ; 9295.05] [13777.14 ; 14141.19]
34	10003.28	0.707082	12794.13	4.180198	0.256 [0.00 ; 9294.32] [13775.69 ; 14190.49]
35	9790.85	0.486185	12768.17	4.215499	0.120 [0.00 ; 9293.60] [13815.57 ; 14189.77]
36	9965.93	0.471244	12762.26	4.213153	0.134 [0.00 ; 9292.87] [13774.96 ; 14189.77]
37	11626.80	1.191479	12795.94	4.060964	0.159 [0.00 ; 9292.87] [13774.24 ; 14189.04]
38	12195.85	1.533889	12794.74	3.947516	0.091 [0.00 ; 9292.87] [13764.81 ; 14239.07]
39	12670.01	3.586949	12874.37	2.258576	0.090 [0.00 ; 9292.15] [13764.09 ; 14239.07]
40	11672.87	0.000000	12733.75	4.236863	0.069 [0.00 ; 9292.15] [13708.26 ; 14337.67]

Table: Parameters for the fit of the dynamic polarizability of the vibrational levels v (with N=0) of the lowest triplet Sigma_u^+ state of Rb_2, using the ansatz of the paper with three effective transitions. omega_eff: effective frequency; d_eff: effective dipole moment.
The frequency ranges taken in account for the fit are indicated as intervals.

#	1st effective transition # v (cm-1)	omega_eff/(2*pi*c) (a.u.)	d_eff (a.u.)	2nd effective transition # v (cm-1)	omega_eff/(2*pi*c) (a.u.)	d_eff (a.u.)	3rd effective transition # v (cm-1)	omega_eff/(2*pi*c) (a.u.)	d_eff (a.u.)	rRMS (%)	frequency domains included in the fit (cm-1)
0	9590.41	0.185198	10120.66	2.785057	13482.52	3.215639	1.071	[0.00 ; 9527.06]	[11017.65 ; 13172.54]	[13698.11 ; 14500.00]	
1	9737.73	0.904303	10217.37	2.641512	13471.82	3.220395	0.830	[0.00 ; 9514.01]	[11172.08 ; 13131.21]	[13719.14 ; 14500.00]	
2	9763.22	1.257521	10333.45	2.488387	13459.98	3.224902	0.860	[0.00 ; 9501.68]	[11239.51 ; 13118.89]	[13724.94 ; 14500.00]	
3	9751.48	1.364655	10430.64	2.426252	13447.38	3.228257	0.860	[0.00 ; 9489.36]	[11332.32 ; 13106.56]	[13738.71 ; 14500.00]	
4	9736.83	1.413862	10524.00	2.391762	13434.65	3.232971	0.917	[0.00 ; 9477.03]	[11396.12 ; 13094.24]	[13792.36 ; 14500.00]	
5	9717.63	1.414144	10602.93	2.386689	13420.99	3.236433	1.019	[0.00 ; 9465.43]	[11483.12 ; 13082.64]	[13765.54 ; 14500.00]	
6	9699.59	1.401748	10677.32	2.389227	13406.69	3.239517	1.163	[0.00 ; 9453.83]	[11567.95 ; 13071.04]	[13761.19 ; 14500.00]	
7	9683.02	1.382871	10748.52	2.395828	13391.70	3.242234	1.162	[0.00 ; 9442.95]	[11648.43 ; 13060.16]	[13766.26 ; 14500.00]	
8	9672.13	1.378077	10831.95	2.391468	13376.86	3.248165	1.366	[0.00 ; 9432.80]	[11683.23 ; 13050.01]	[13803.97 ; 14500.00]	
9	9655.95	1.341866	10891.17	2.410047	13359.86	3.247776	0.911	[0.00 ; 9422.65]	[11780.39 ; 13039.86]	[13794.54 ; 14500.00]	
10	9647.39	1.330426	10972.00	2.409608	13343.58	3.253083	0.921	[0.00 ; 9413.23]	[11812.29 ; 13030.43]	[13775.69 ; 14500.00]	
11	9637.84	1.308216	11044.01	2.417081	13326.02	3.255710	1.123	[0.00 ; 9403.80]	[11863.77 ; 13021.01]	[13766.99 ; 14500.00]	
12	9641.33	1.333716	11171.09	2.368223	13317.41	3.292024	0.711	[0.00 ; 9394.38]	[11933.37 ; 13011.58]	[13774.96 ; 14340.57]	
13	9630.35	1.300184	11251.03	2.376126	13300.81	3.305618	0.650	[0.00 ; 9385.68]	[11999.35 ; 13002.88]	[13774.96 ; 14331.87]	
14	9619.82	1.264942	11330.84	2.383139	13284.29	3.320739	0.717	[0.00 ; 9377.70]	[12044.30 ; 12986.93]	[13774.96 ; 14273.87]	
15	9611.72	1.230969	11398.49	2.394595	13264.85	3.324882	0.672	[0.00 ; 9369.73]	[12088.53 ; 12965.91]	[13812.67 ; 14315.92]	
16	9611.41	1.220352	11494.21	2.371852	13250.66	3.349338	0.794	[0.00 ; 9362.48]	[12146.53 ; 12941.25]	[13769.16 ; 14258.65]	
17	9602.28	1.178701	11560.85	2.385153	13230.57	3.356448	0.760	[0.00 ; 9355.23]	[12186.41 ; 12921.68]	[13798.89 ; 14252.12]	
18	9600.19	1.154154	11638.84	2.378668	13212.05	3.369833	0.746	[0.00 ; 9348.70]	[12239.34 ; 12899.20]	[13801.07 ; 14245.59]	
19	9599.30	1.130792	11723.85	2.363649	13193.91	3.390178	0.815	[0.00 ; 9342.90]	[12289.36 ; 12884.70]	[13776.41 ; 14239.07]	
20	9611.89	1.132451	11808.64	2.330800	13176.30	3.406338	0.698	[0.00 ; 9336.37]	[12349.54 ; 12852.80]	[13770.61 ; 14233.27]	
21	9589.93	1.055503	11864.09	2.362846	13153.04	3.416474	0.760	[0.00 ; 9331.30]	[12368.39 ; 12847.72]	[13793.09 ; 14177.44]	
22	9593.22	1.030744	11936.50	2.352384	13131.44	3.427758	0.661	[0.00 ; 9326.22]	[12422.05 ; 12828.87]	[13807.59 ; 14172.37]	
23	9610.59	1.028859	12011.99	2.318529	13111.74	3.443508	0.578	[0.00 ; 9321.15]	[12460.47 ; 12804.95]	[13793.09 ; 14218.04]	
24	9608.67	0.986896	12075.04	2.314174	13089.46	3.457836	0.571	[0.00 ; 9317.52]	[12485.85 ; 12794.07]	[13789.46 ; 14213.69]	
25	9611.16	0.949278	12136.81	2.302735	13068.36	3.474431	0.444	[0.00 ; 9313.17]	[12519.93 ; 12770.15]	[13804.69 ; 14109.29]	
26	9630.08	0.932263	12196.63	2.283813	13045.34	3.483366	0.363	[0.00 ; 9309.55]	[12551.83 ; 12705.57]	[13811.94 ; 14156.42]	
27	9652.31	0.914930	12265.06	2.248322	13022.47	3.505861	0.348	[0.00 ; 9306.65]	[12588.08 ; 12744.77]	[13788.74 ; 14152.79]	
28	9664.11	0.875433	12323.33	2.239643	12997.09	3.517888	0.244	[0.00 ; 9303.75]	[12647.53 ; 12722.29]	[13815.57 ; 14099.86]	
29	9713.59	0.873735	12370.71	2.194975	12977.59	3.537408	0.326	[0.00 ; 9301.57]	[12651.88 ; 12703.44]	[13773.51 ; 14147.71]	
30	9462.31	0.438363	11672.79	2.320231	13035.17	3.508957	0.213	[0.00 ; 9299.40]	[12684.51 ; 12695.47]	[13780.76 ; 14145.54]	
31	9549.01	0.536731	12413.74	3.394454	13188.14	2.485224	0.029	[0.00 ; 9297.95]	[13769.16 ; 14144.09]		
32	9549.37	0.485334	12477.46	3.502939	13180.90	2.340804	0.025	[0.00 ; 9296.50]	[13768.44 ; 14142.64]		
33	9549.31	0.431667	12537.24	3.627132	13177.05	2.154360	0.021	[0.00 ; 9295.05]	[13777.14 ; 14141.19]		
34	9547.69	0.375099	12592.55	3.771700	13182.21	1.901211	0.018	[0.00 ; 9294.32]	[13775.69 ; 14190.49]		
35	9546.97	0.318713	12648.01	3.952470	13215.83	1.501938	0.016	[0.00 ; 9293.60]	[13815.57 ; 14189.77]		
36	9267.78	0.000000	11274.59	1.182139	12810.47	4.060789	0.240	[0.00 ; 9292.87]	[13774.96 ; 14189.77]		
37	9515.30	0.188211	12709.74	4.169399	13316.67	0.743190	0.018	[0.00 ; 9292.87]	[13774.24 ; 14189.04]		
38	9386.63	0.082332	12648.45	3.652151	12944.33	2.146721	0.045	[0.00 ; 9292.87]	[13764.81 ; 14239.07]		
39	9193.98	0.000000	12724.88	4.221117	13355.56	0.374808	0.043	[0.00 ; 9292.15]	[13764.09 ; 14239.07]		
40	9596.83	0.000000	12731.90	4.235114	13550.10	0.110491	0.071	[0.00 ; 9292.15]	[13708.26 ; 14337.67]		

Table: Parameters for the fit of the dynamic polarizability of the vibrational levels v (with N=0) of the lowest singlet Sigma_g^+ state of Rb_2, using the ansatz of the paper with two effective transitions. omega_eff: effective frequency; d_eff: effective dipole moment.
The frequency ranges taken in account for the fit are indicated as intervals.

#	1st effective transition # v omega_eff/(2*pi*c)	d_eff (cm-1)	2nd effective transition omega_eff/(2*pi*c)	d_eff (a.u.)	rms (%)	frequency domains included in the fit (cm-1)
0	11450.31	2.647731	15019.57	2.965774	0.518	[0.00 ; 9432.03] [9959.90 ; 10613.49] [12889.62 ; 14736.22] [15817.69 ; 16000.00]
1	11383.24	2.689551	14963.22	2.929415	1.962	[0.00 ; 9375.10] [9959.07 ; 10556.56] [12980.37 ; 14679.29] [15880.39 ; 16000.00]
2	11263.16	2.707908	14893.80	2.828507	2.175	[0.00 ; 9319.00] [10071.28 ; 10499.63] [13069.48 ; 14623.19] [15979.40 ; 16000.00]
3	11192.67	2.726587	14841.26	2.774923	1.770	[0.00 ; 9262.90] [10014.35 ; 10365.15] [13232.01 ; 14567.09]
4	11084.86	2.738700	14793.77	2.724816	2.423	[0.00 ; 9263.72] [10069.63 ; 10358.55] [13241.09 ; 14510.98]
5	10988.23	2.746025	14752.23	2.688516	2.736	[0.00 ; 9207.62] [10124.91 ; 10302.45] [13359.07 ; 14454.88]
6	10896.90	2.743087	14716.89	2.665019	3.174	[0.00 ; 9209.27] [10124.05 ; 10247.17] [13630.51 ; 14399.60]
7	11177.30	2.815120	14700.93	2.730883	0.827	[0.00 ; 9210.92] [13517.48 ; 14344.32]
8	11147.88	2.830717	14669.19	2.716210	0.776	[0.00 ; 9155.64] [13529.03 ; 14289.05]
9	11106.07	2.845253	14637.00	2.696263	0.816	[0.00 ; 9158.12] [13571.93 ; 14234.59]
10	11059.13	2.858737	14604.95	2.675684	0.889	[0.00 ; 9159.77] [13585.13 ; 14180.14]
11	11010.69	2.871102	14573.62	2.654337	0.986	[0.00 ; 9162.24] [13624.73 ; 14126.51]
12	10970.15	2.878189	14547.88	2.646632	1.012	[0.00 ; 9108.61] [13819.44 ; 14072.89]
13	10838.51	2.793461	14587.80	2.757705	1.008	[0.00 ; 9111.09] [13886.27 ; 14019.26]
14	10881.05	2.890135	14500.45	2.627477	1.117	[0.00 ; 9058.29] [13745.19 ; 13966.46]
15	10727.35	2.799699	14543.51	2.741307	1.213	[0.00 ; 9116.86] [13812.02 ; 13959.03]
16	10208.21	2.257552	14978.89	3.404092	0.226	[0.00 ; 9119.34] [13845.02 ; 13906.23]
17	10002.85	1.947713	13849.09	3.524078	0.024	[0.00 ; 9122.64]
18	10100.47	2.224233	14911.39	3.438765	0.160	[0.00 ; 9070.66] [13855.74 ; 13893.03]
19	10061.69	2.225589	14922.86	3.445085	0.122	[0.00 ; 9018.68] [13835.12 ; 13841.87]
20	9882.99	1.945188	13777.83	3.534547	0.027	[0.00 ; 9078.09]
21	9843.10	1.941773	13738.67	3.538702	0.030	[0.00 ; 9081.39]
22	9813.35	1.953855	13746.87	3.537403	0.028	[0.00 ; 9030.23]
23	9777.20	1.948963	13708.85	3.541736	0.031	[0.00 ; 9034.36]
24	9750.04	1.960652	13717.97	3.540422	0.028	[0.00 ; 8984.86]
25	9708.16	1.942813	13630.49	3.548562	0.038	[0.00 ; 9042.61]
26	9676.11	1.939030	13590.00	3.551851	0.042	[0.00 ; 9046.73]
27	9645.62	1.935171	13549.82	3.554939	0.047	[0.00 ; 9050.04]
28	9624.18	1.952327	13569.55	3.551978	0.042	[0.00 ; 9001.36]
29	9588.19	1.934617	13470.93	3.558445	0.057	[0.00 ; 9052.51]
30	9562.35	1.934546	13435.34	3.559923	0.062	[0.00 ; 9050.86]
31	9545.37	1.953333	13466.08	3.556637	0.054	[0.00 ; 9003.01]
32	9515.47	1.940706	13378.95	3.560743	0.069	[0.00 ; 9039.31]
33	9493.89	1.943129	13349.76	3.561133	0.073	[0.00 ; 9035.18]
34	9473.56	1.945944	13322.16	3.561295	0.078	[0.00 ; 9031.06]
35	9456.33	1.956178	13318.38	3.559747	0.077	[0.00 ; 9014.56]
36	9437.75	1.960584	13288.73	3.559217	0.082	[0.00 ; 9013.73]
37	9424.53	1.972904	13301.55	3.557346	0.078	[0.00 ; 8990.63]
38	9407.51	1.976326	13267.29	3.556797	0.084	[0.00 ; 8994.76]
39	9392.40	1.983139	13243.85	3.555443	0.088	[0.00 ; 8993.93]
40	9381.54	1.996441	13253.11	3.553087	0.085	[0.00 ; 8977.43]
41	9375.86	2.021790	13313.92	3.548456	0.070	[0.00 ; 8932.88]
42	9356.73	2.009166	13209.66	3.550194	0.093	[0.00 ; 8980.73]
43	9358.74	2.052830	13346.77	3.542223	0.062	[0.00 ; 8895.75]
44	9338.83	2.029753	13201.80	3.545753	0.094	[0.00 ; 8971.66]
45	9336.82	2.058367	13275.94	3.540565	0.075	[0.00 ; 8928.75]
46	9339.36	2.096092	13393.08	3.533154	0.052	[0.00 ; 8848.72]
47	9333.18	2.106903	13392.40	3.530663	0.051	[0.00 ; 8847.90]
48	9323.64	2.103332	13337.80	3.531068	0.062	[0.00 ; 8886.68]
49	9318.98	2.116007	13338.47	3.527961	0.062	[0.00 ; 8887.50]
50	9315.02	2.125330	13333.24	3.525646	0.063	[0.00 ; 8893.28]
51	9314.11	2.141766	13357.85	3.521955	0.058	[0.00 ; 8880.08]
52	9311.93	2.151245	13356.64	3.519599	0.058	[0.00 ; 8885.03]
53	9310.18	2.163034	13354.05	3.516491	0.059	[0.00 ; 8892.45]
54	9314.05	2.185063	13415.45	3.511925	0.048	[0.00 ; 8852.85]
55	9317.92	2.205836	13467.32	3.507238	0.039	[0.00 ; 8814.07]
56	9318.38	2.215597	13465.81	3.504802	0.039	[0.00 ; 8822.32]
57	9321.95	2.231658	13494.15	3.500965	0.035	[0.00 ; 8801.70]
58	9322.50	2.236386	13472.81	3.499704	0.038	[0.00 ; 8829.75]
59	9325.20	2.246586	13474.43	3.497270	0.038	[0.00 ; 8833.87]
60	9332.11	2.265347	13521.61	3.492997	0.031	[0.00 ; 8790.97]
61	9335.86	2.272377	13517.88	3.491465	0.031	[0.00 ; 8798.40]
62	9342.86	2.287969	13551.11	3.487904	0.026	[0.00 ; 8762.10]
63	9345.01	2.287936	13512.58	3.488343	0.031	[0.00 ; 8805.82]
64	9355.62	2.306927	13573.27	3.483989	0.023	[0.00 ; 8731.57]
65	9361.08	2.313513	13564.84	3.483078	0.023	[0.00 ; 8736.52]
66	9364.38	2.310490	13521.05	3.485027	0.028	[0.00 ; 8780.25]
67	9373.19	2.320842	13540.44	3.483386	0.024	[0.00 ; 8746.42]
68	9382.32	2.330355	13554.17	3.482087	0.021	[0.00 ; 8714.24]
69	9383.40	2.317073	13471.50	3.487990	0.030	[0.00 ; 8789.32]
70	9395.20	2.329938	13508.42	3.486106	0.024	[0.00 ; 8730.74]
71	9401.64	2.326841	13477.73	3.489506	0.025	[0.00 ; 8742.29]
72	9407.54	2.321753	13440.51	3.493896	0.028	[0.00 ; 8756.32]
73	9415.13	2.318271	13418.38	3.498014	0.028	[0.00 ; 8752.20]
74	9425.64	2.320938	13419.16	3.500383	0.025	[0.00 ; 8723.32]
75	9429.20	2.305132	13355.00	3.509545	0.030	[0.00 ; 8755.50]
76	9442.08	2.309778	13371.57	3.511674	0.025	[0.00 ; 8709.29]
77	9447.61	2.295936	13322.42	3.520967	0.028	[0.00 ; 8724.14]
78	9452.64	2.279567	13271.63	3.531566	0.030	[0.00 ; 8738.17]
79	9466.62	2.281567	13287.09	3.535311	0.025	[0.00 ; 8689.49]
80	9468.05	2.254515	13211.08	3.550865	0.030	[0.00 ; 8725.79]

81	9473.88	2.235088	13166.77	3.563714	0.032	[0.00 ; 8730.74]
82	9484.27	2.224975	13157.22	3.572906	0.029	[0.00 ; 8705.99]
83	9487.26	2.196832	13098.00	3.589895	0.032	[0.00 ; 8724.14]
84	9497.46	2.183098	13087.81	3.600874	0.030	[0.00 ; 8700.22]
85	9513.36	2.179872	13105.63	3.607725	0.024	[0.00 ; 8645.76]
86	9517.28	2.149908	13059.28	3.625901	0.025	[0.00 ; 8655.67]
87	9519.21	2.113937	13006.38	3.646556	0.027	[0.00 ; 8672.99]
88	9511.69	2.057523	12915.59	3.675471	0.034	[0.00 ; 8727.44]
89	9529.57	2.051950	12941.50	3.683968	0.027	[0.00 ; 8669.69]
90	9529.37	2.009042	12894.41	3.707103	0.029	[0.00 ; 8687.02]
91	9528.63	1.962363	12846.68	3.731797	0.031	[0.00 ; 8705.99]
92	9545.70	1.950943	12869.57	3.742245	0.025	[0.00 ; 8650.72]
93	9553.80	1.918367	12856.44	3.761154	0.023	[0.00 ; 8633.39]
94	9551.50	1.866579	12816.63	3.786906	0.024	[0.00 ; 8653.19]
95	9537.66	1.792444	12748.78	3.820251	0.029	[0.00 ; 8711.77]
96	9544.41	1.753703	12742.39	3.840335	0.027	[0.00 ; 8696.92]
97	9561.03	1.732331	12763.41	3.853660	0.022	[0.00 ; 8644.94]
98	9544.53	1.650799	12706.31	3.887472	0.026	[0.00 ; 8706.82]
99	9561.88	1.625137	12727.86	3.901814	0.021	[0.00 ; 8655.67]
100	9555.12	1.559982	12702.97	3.928275	0.022	[0.00 ; 8681.24]
101	9548.67	1.492998	12681.93	3.954403	0.023	[0.00 ; 8705.17]
102	9553.27	1.441929	12683.00	3.974922	0.021	[0.00 ; 8694.44]
103	9580.44	1.420738	12716.85	3.986278	0.015	[0.00 ; 8611.94]
104	9595.33	1.378012	12729.22	4.003254	0.012	[0.00 ; 8565.74]
105	9552.23	1.259510	12675.30	4.039337	0.017	[0.00 ; 8705.17]
106	9568.39	1.215614	12693.19	4.054950	0.014	[0.00 ; 8659.79]
107	9558.89	1.139750	12685.56	4.077061	0.014	[0.00 ; 8691.14]
108	9572.52	1.088815	12699.79	4.092563	0.011	[0.00 ; 8654.84]
109	9577.94	1.026769	12706.26	4.109467	0.010	[0.00 ; 8642.46]
110	9554.84	0.936267	12695.11	4.130496	0.011	[0.00 ; 8712.59]
111	9557.79	0.871677	12702.17	4.145328	0.009	[0.00 ; 8709.29]
112	9561.12	0.806703	12709.11	4.159077	0.008	[0.00 ; 8705.17]
113	9564.72	0.741371	12715.78	4.171734	0.007	[0.00 ; 8702.69]
114	9568.55	0.676546	12722.10	4.183155	0.006	[0.00 ; 8700.22]
115	9573.17	0.612471	12728.23	4.193373	0.005	[0.00 ; 8697.74]
116	9578.47	0.549063	12734.02	4.202418	0.004	[0.00 ; 8696.09]
117	9584.65	0.486356	12739.48	4.210336	0.003	[0.00 ; 8695.27]
118	9594.62	0.425485	12744.70	4.217095	0.003	[0.00 ; 8694.44]
119	9577.09	0.354456	12746.11	4.223570	0.003	[0.00 ; 8761.27]
120	9636.94	0.310253	12752.36	4.227532	0.002	[0.00 ; 8692.79]
121	9655.62	0.251670	12753.80	4.232437	0.002	[0.00 ; 8760.45]
122	9806.04	0.220488	12756.29	4.235328	0.001	[0.00 ; 8760.45]
123	10319.14	0.248531	12761.67	4.234457	0.001	[0.00 ; 8760.45]
124	12073.63	1.115818	12809.17	4.092981	0.003	[0.00 ; 8760.45]